

Structural Materials: New Challenges, Manufacturing and Performance

Baldev Raj

Indira Gandhi Centre for Atomic Research,
Kalpakkam 603 102, INDIA
E-mail: dir@igcar.gov.in, www.igcar.gov.in

Asayama Tai

Japan Atomic Energy Agency (JAEA), Ibaraki, JAPAN

Fazio Concetta

Karlsruhe Institute of Technology (KIT), Programm NUKLEAR, GERMANY

FR09 -International Conference on Fast Reactors and Related Fuel Cycles
- Challenges and Opportunities - December 7 - 11, 2009, Kyoto, Japan

WORLD FAST REACTORS: SCENARIO

Interest in FBR has been renewed internationally

- Sustainable nuclear power
 - Effective utilisation of uranium resources
 - Burning of minor actinides: reduction of waste volume and toxicity
- China, France, India, Japan, Korea, Russia, and USA have interest in Fast Reactors (FR)
 - France, Japan, and USA have signed an MOU to cooperate under the Global Nuclear Energy (GNEP) Partnership to demonstrate the feasibility of the sodium-cooled fast reactor technology to accomplish sustainability requirements
 - International collaborative programmes on innovative reactors such as Generation-IV & INPRO are focusing on FRs
 - 390 reactor years operating experience including test reactors

INDIA
(IGCAR)

JAPAN
(FaCT)

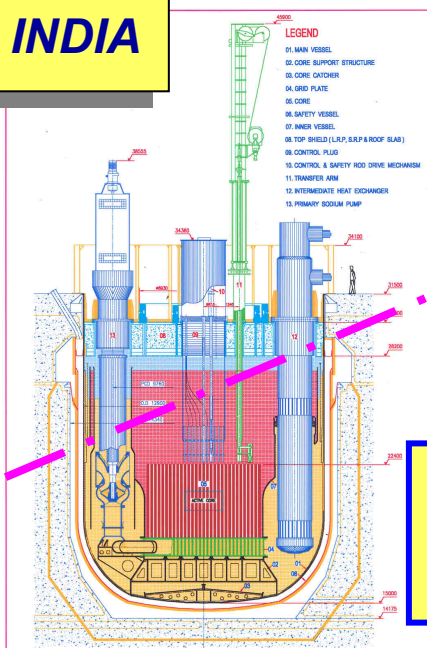
European
Commission
(GETMAT)

Baldev Raj, A. Vasile, V. Kagramanian, m. Xu, R. nakai, Y.I. Kim, F. Depisch and A. Stanculescu – Assessment of compatibility of a system with fast reactors with sustainability, Paper being presented at this international conference(FR-09)

Road map of fast reactors in INDIA

21 GWe by 2020
275 GWe by 2052

Fast Breeder Test Reactor



4 more FBRs before 2020

Metal fuelled FBR by 2020
High Breeding Ratio

500 MWe Fast Breeder Reactor (2011)

Operating since 1985
• 40 MWth nominal capacity
• (U,Pu)C fuel – First time in the world
• Mark-I reached a burn-up – 165 GWd/t

Fast Reactors: Roadmap

Road map of fast reactors in JAPAN

Commercial Plants in around 2050

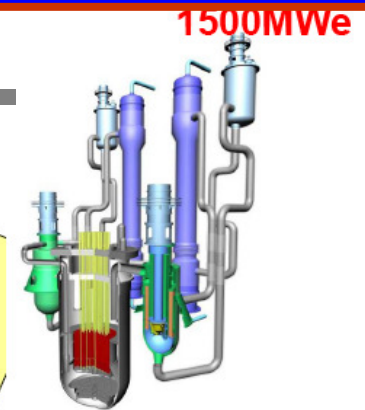
Experimental Reactor JOYO

Criticality in 1977
140 MWth
Operation hour: over 70,000



Prototype Power Reactor MONJU

Criticality in 1993
280 MWe



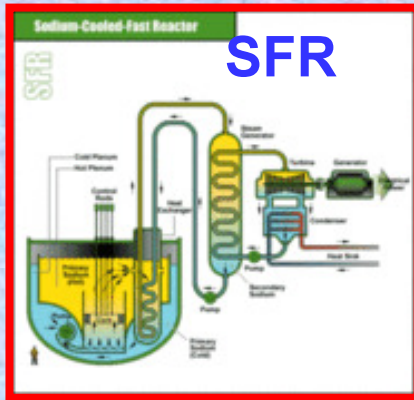
Demonstration Plant

Start Operation ~ 2025
500-750 MWe

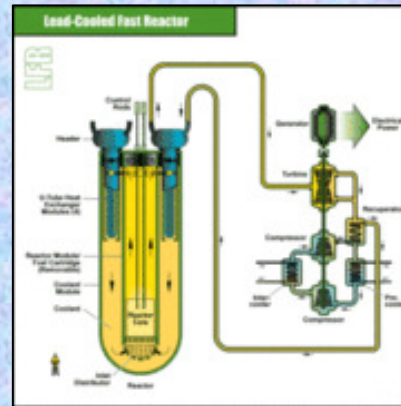
The subject of this presentation

GENERATION IV INTERNATIONAL FORUM

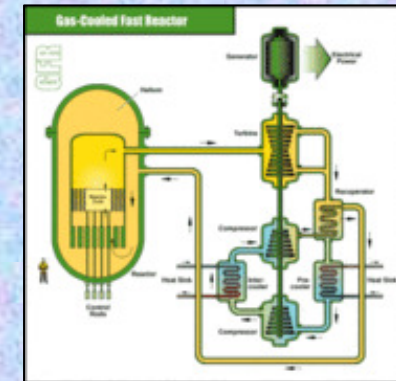
IMPROVE NUCLEAR SAFETY, PROLIFERATION RESISTANT DESIGNS;
MINIMISE WASTE; MAXIMISE RESOURCE UTILISATION;
DECREASE COST OF CONSTRUCTION AND MAINTENANCE;



SODIUM COOLED FAST REACTOR
 Primary choice



GAS COOLED FAST REACTOR



LEAD COOLED FAST REACTOR

| Reactor System | Coolant | Neutron Spectrum | Core Outlet Temp (°C) |
|-------------------------------|-------------------------------|------------------|-----------------------|
| Gas Cooled Fast Reactor (GFR) | Gas (e.g. He) | Fast | ~850 |
| Lead-Cooled Reactor (LFR) | Liquid Metal (e.g. Pb, Pb-Bi) | Fast | 550-800 |
| SFR (LMFBR) | Liquid Metal (Na) | Fast | ~550 |

Materials Challenges for SFR

Material Targets

Higher Burn-up:

10-12 at% to 20-30 at%

• Longer Operating Life

20 to 40 to 60 years

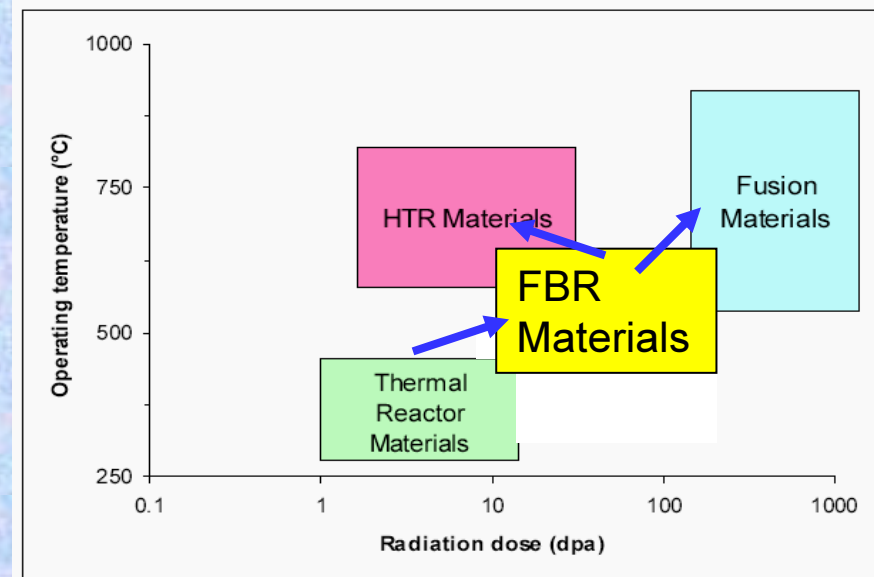
Higher Operating Temp

550° C to 600° C to 700° C

Higher Breeding Ratio

1.1 to 1.45

Higher transmutation of actinides long lived fission product separation



Effective material development strategy

- ✓ Alloy development and characterisation
- ✓ Compatibility with coolant, Sodium: Modelling and validation
- ✓ Improvement and extension of the knowledge base for qualification of materials; improvement in codes
- ✓ Joining and welding : New process, Modelling and performance
- ✓ Development of corrosion protection barriers;
- ✓ Development of advanced NDE and inspection technologies;
- ✓ Improved modelling techniques and experimental validation.

Material Issues in Fast Reactor Components

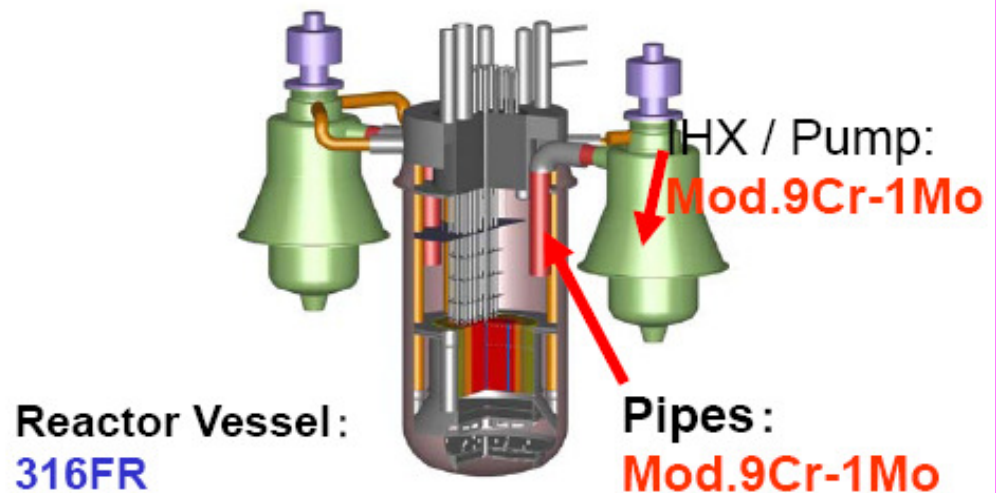
| | | |
|---------------------------------|---|---|
| Core | <ul style="list-style-type: none"> • Cold Worked 316 SS • 15%Cr-15%Ni-Ti stabilized SS-D9 & its variants • Ferritic-Martensitic Steels (Mod. 9Cr-1Mo, ODS) | <ul style="list-style-type: none"> • Radiation damage • High temperature mechanical properties • Compatibility with sodium, fuel & fission products • Tribology |
| Structural materials | <ul style="list-style-type: none"> ➤ SS 316 L or 316 LN | <ul style="list-style-type: none"> ➤ Tensile strength ➤ Creep ➤ Low cycle fatigue ➤ Weldability & fabricability ➤ Ratcheting ➤ Thermo-mechanical fatigue ➤ Tribology |
| Steam Generator/ Turbine | <ul style="list-style-type: none"> ✓ Ferritic-martensitic steels | <ul style="list-style-type: none"> ✓ Compatibility with sodium and steam, ✓ Resistance to corrosion, fretting and wear |

Baldev Raj, et al (2008) *Approaches to Development of Steels and Manufacturing Technologies for Fusion Reactors*, in "Energy Materials: Advances in Characterization, Modelling and Application" ed(s) Andersen, N.H.; Eldrup, M.; Hansen, N.; Juul Jensen, D.; Nielsen, E.M.; Nielsen, S.F.; Sørensen, B.F.; Pedersen, A.S.; Vegge, T.; West, S.S.; Pages 123-1452

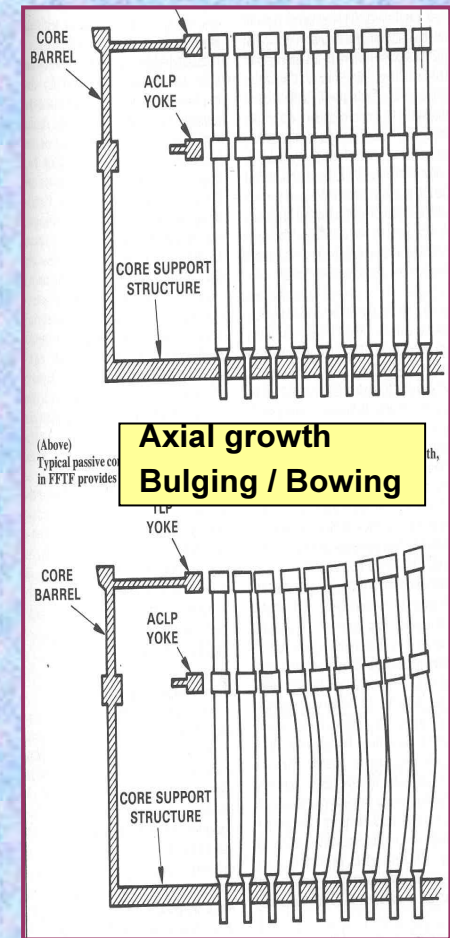
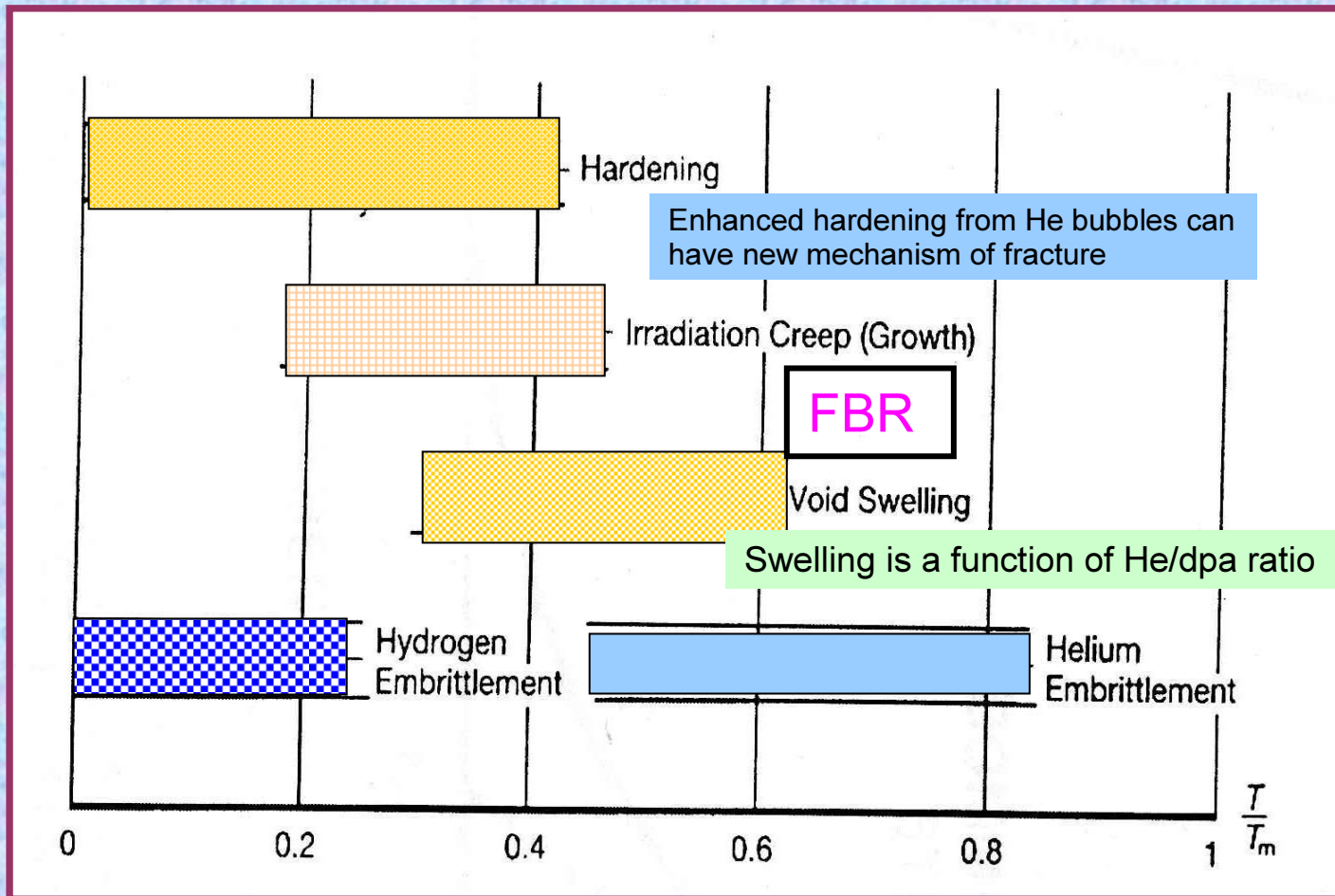
Materials for Fast Reactors: International

| Components | India | Japan (FaCT) | Europe |
|------------------------------|---|---|---------------------|
| Core | CW 15%Cr-15%Ni- Ti,P SS-D9 & its variants for both clad and wrapper (130 dpa) | ODS steel clad | 9-12 Cr ODS as clad |
| | ODS clad & Ferritic-Martensitic Steels wrapper (Mod. 9Cr-1Mo)(170 dpa) | PNC-FMS(11Cr ferritic steel) wrapper with SUS 316 joint | 9-12 Cr F/M steels |
| Reactor vessel and internals | SS 316 L or 316 LN | 316 FR(C: -0.02 (wt%) N: 0.06-0.12 P: 0.02-0.045) | 9-12Cr F/M |
| SG / Turbine | Ferritic-martensitic steels | Mod 9Cr-1Mo | 9-12Cr F/M |

Convergence towards 9-12 Cr F/M steels for wrapper, 9-12 Cr ODS as clad, 316 LN or 316 FR for reactor vessel and internals



Radiation damage effects in reactor structural materials

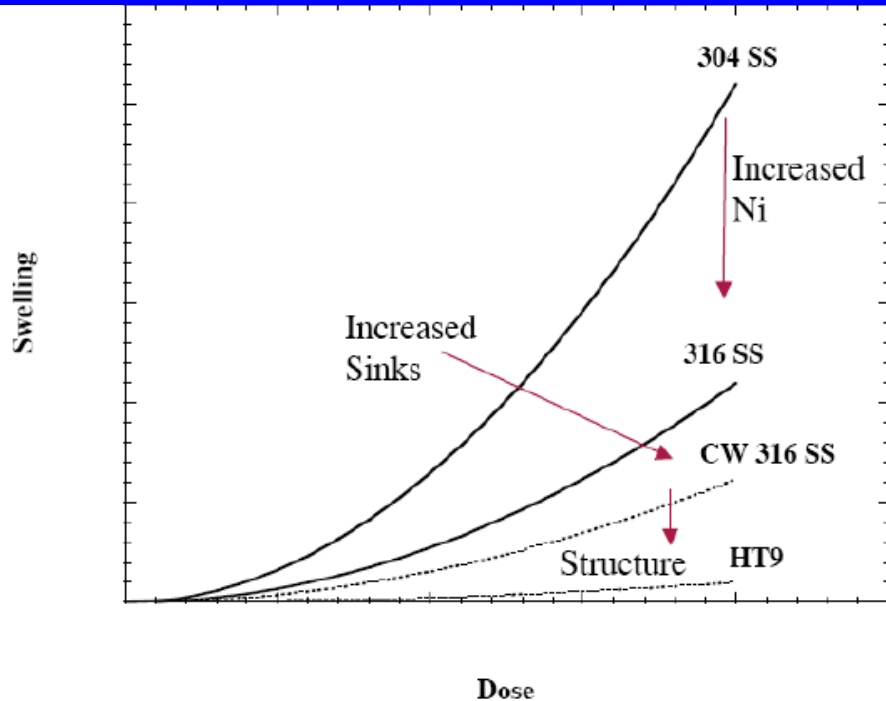


Temperature range (normalized to the melting point T_m)

Dimensional changes due to Swelling and Creep limit the residence time of fuel sub-assembly: Increase in residence time reduces unit cost of power

Control of chemical composition, nanoscale precipitates and particles can reduce both swelling and high temperature embrittlement

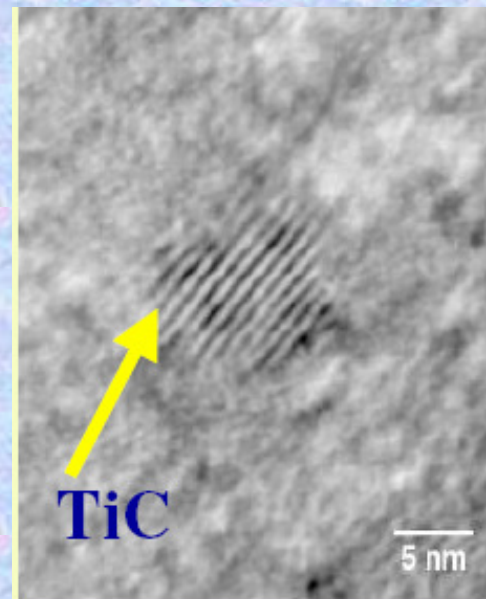
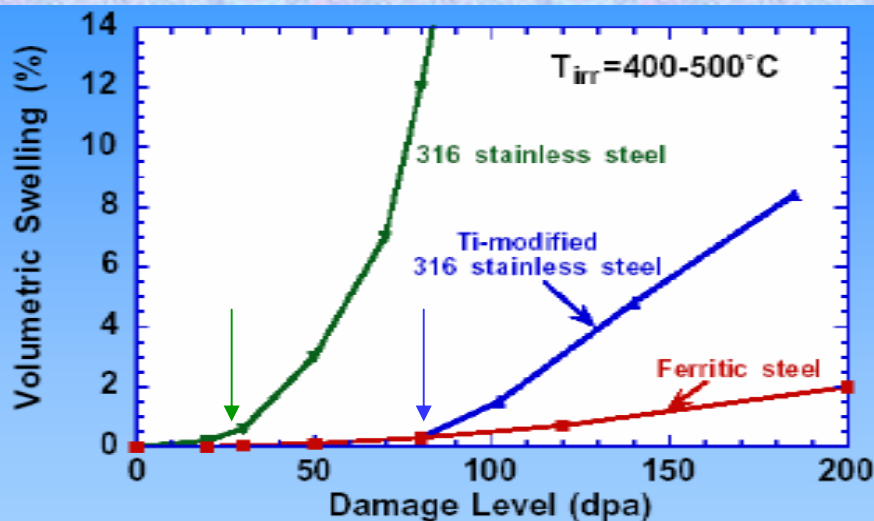
Swelling Resistance Improvement (extending incubation period and reduce rate of swelling in transient region)



-Increase Ni and Decrease Cr;
(increases vacancy diffusion Coefficient)

Optimize Cold work (Reduce effective bias of dislocations)

-Small additions of Ti (Ti/C : 4-8); formation of fine coherent TiC ppt. provide sites for recombination)

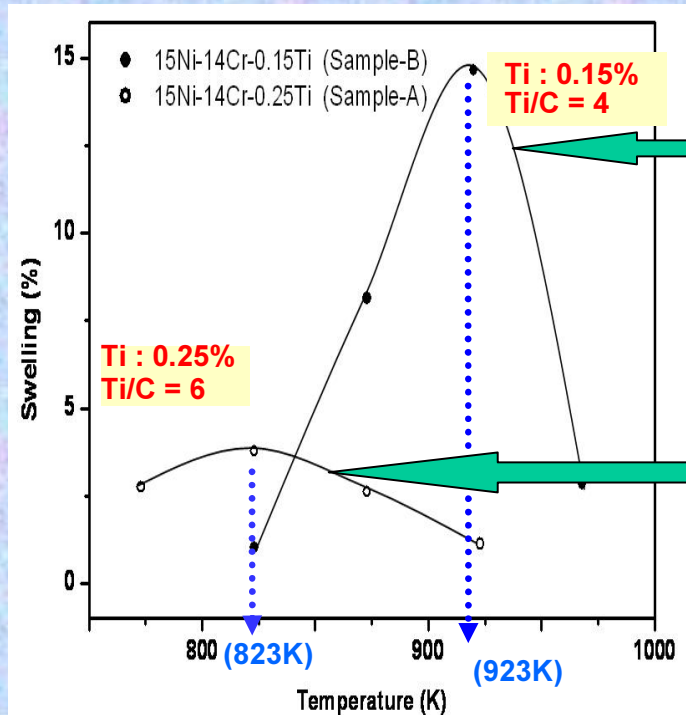


HREM lattice image showing fine scale coherent TiC precipitates – Contribute to improved void swelling resistance and creep properties

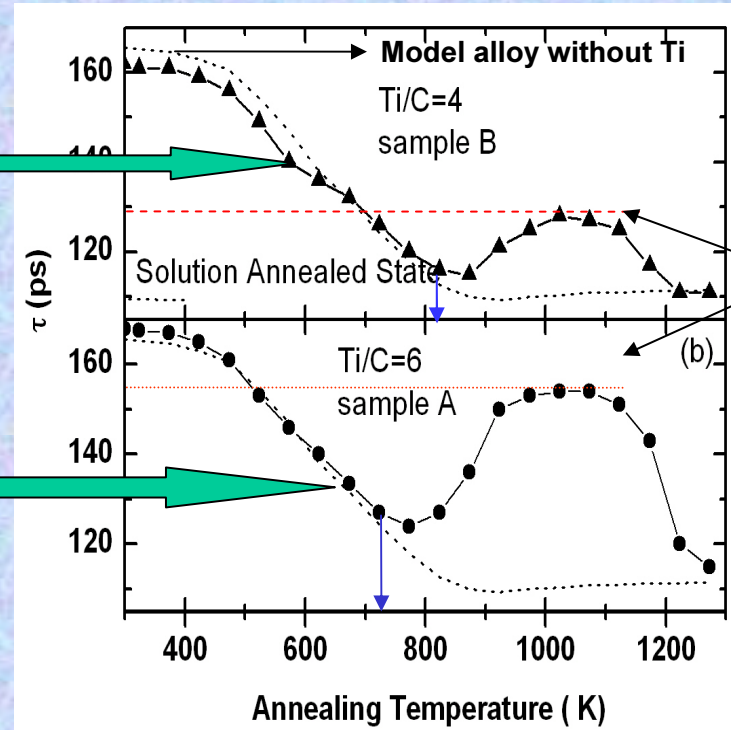


Void Swelling and Positron Annihilation Studies on 20% CW D9 Alloy with 0.15 and 0.25% Ti

Swelling studies at 100 dpa



Positron Annihilation studies

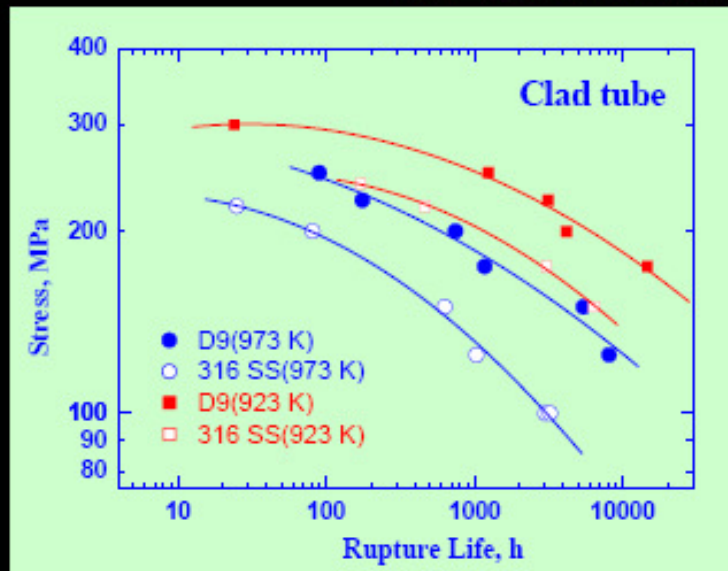


TiC precipitates: The increase in average lifetime of positrons is due to the increase in the number density of TiC precipitates (beyond 750 K in Sample A and beyond 850 K in Sample B), which are effective in reducing the swelling. Thus, the swelling at Peak swelling temperature is less in sample A (Ti/C=6). Also, the shift in peak swelling temperature is also correlated with the onset of TiC precipitation.

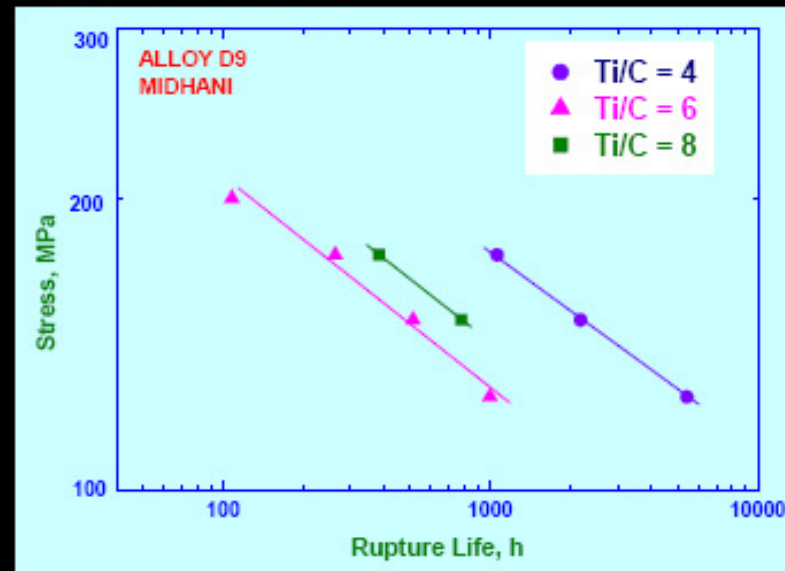
Ti in solution: At lower temperatures, where TiC has not yet formed, Ti in solution enhances vacancy diffusivity and hence, promotes swelling - Sample A has higher swelling than sample B (for temperatures < 850 K).



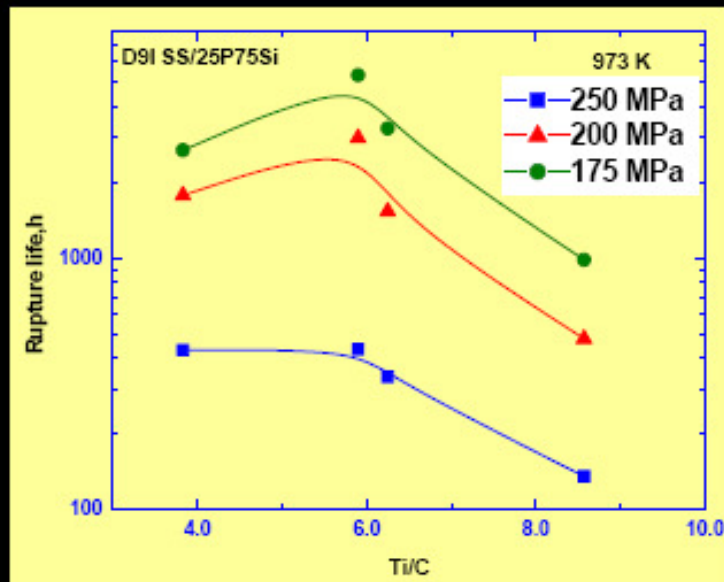
316 ---> D9 --> D9I : CORE MATERIAL DEVELOPMENT- MECHANICAL PROPERTIES



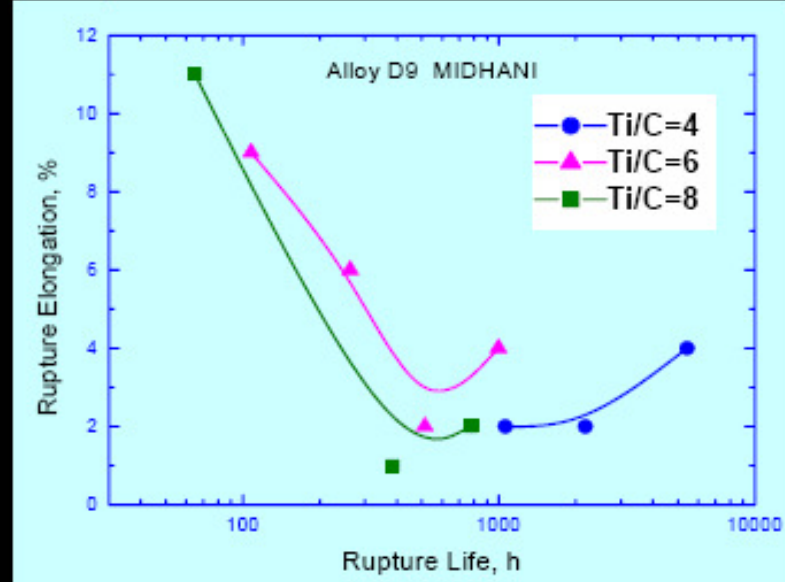
Comparison of 316 SS and D9 SS



Optimisation of D9 SS wrt Ti/C



Ti/C optimisation of D9I

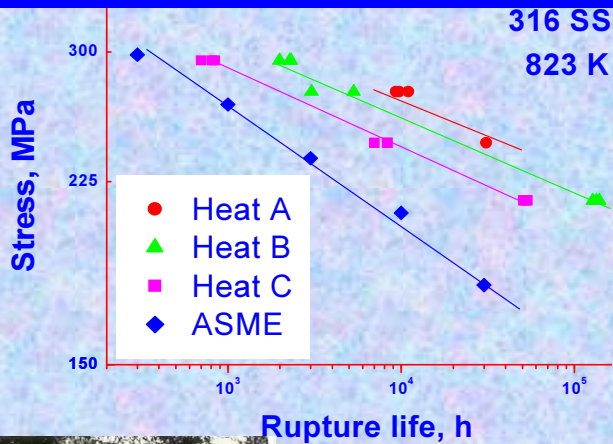


Optimisation of D9 SS wrt Ti/C

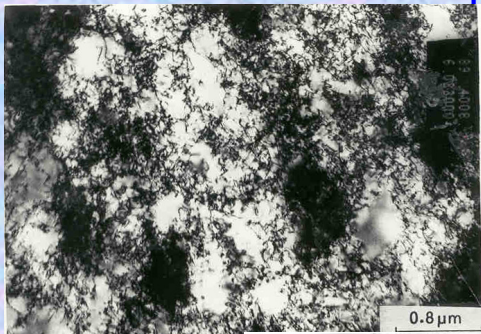
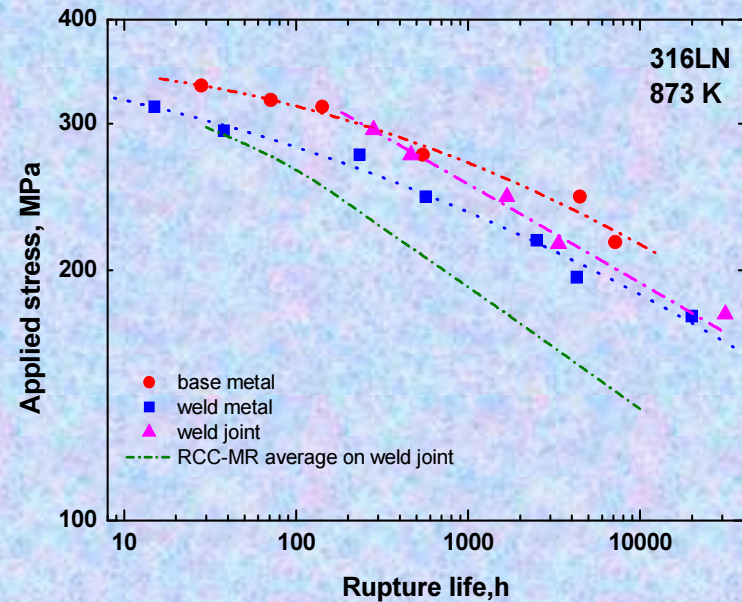


Creep Properties, Deformation and Damage in Stainless Steels and Welds

Heat to heat variation in 316 SS

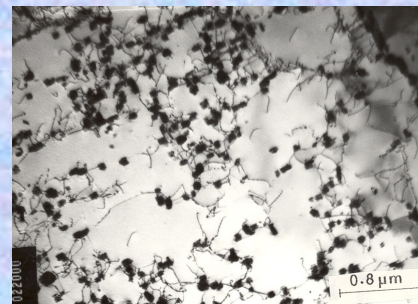


Relative strength of 316 LN SS base, weld and weld joint



823 K, 700 h

Cell structure at 823 K



873 K, 22000 h

uniform distribution of dislocations anchored by ppts.

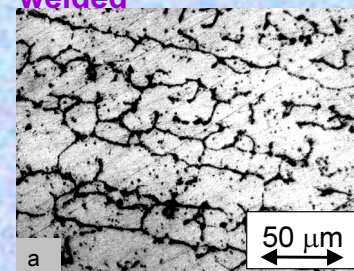
923 K, 1000 h



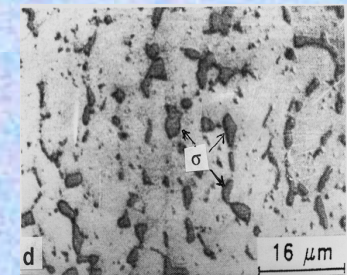
Subgrain development at 923 K

Substructural evolution in 316 SS

δ -ferrite, as welded



σ -phase 923 K, 5400 h



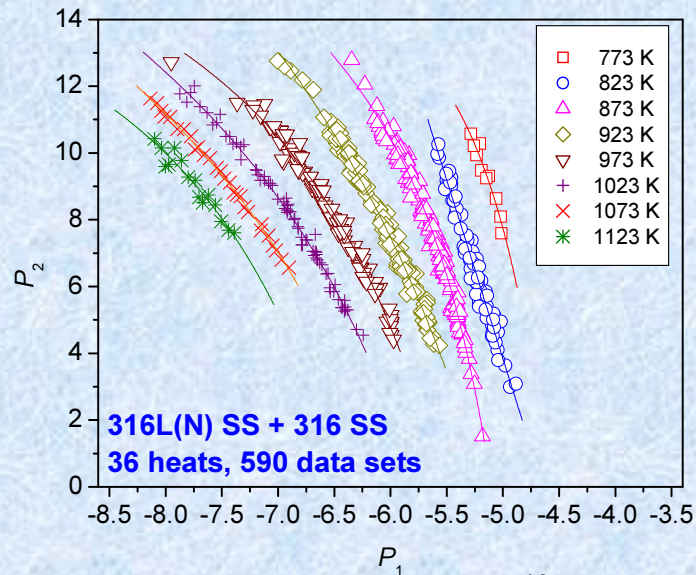
Microstructural stability of welds

Identification of deformation and damage mechanisms led to accurate extrapolation of creep data for longer creep rupture lives of PFBR components



Stress rupture correlation accounting heat-to-heat variation

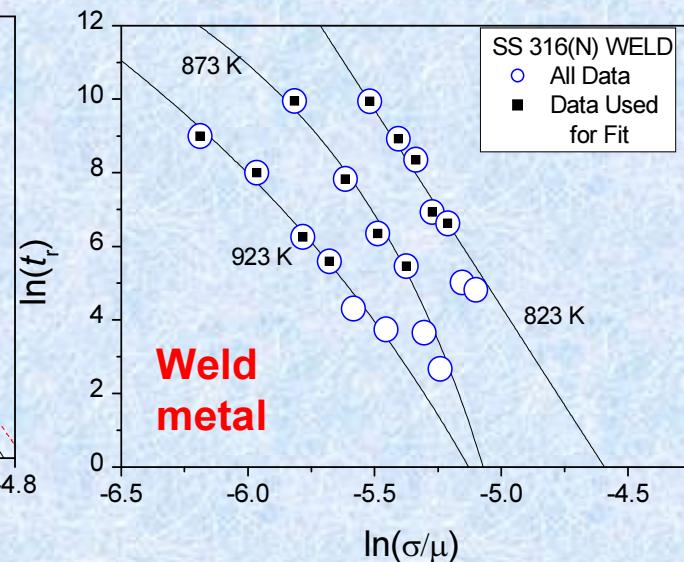
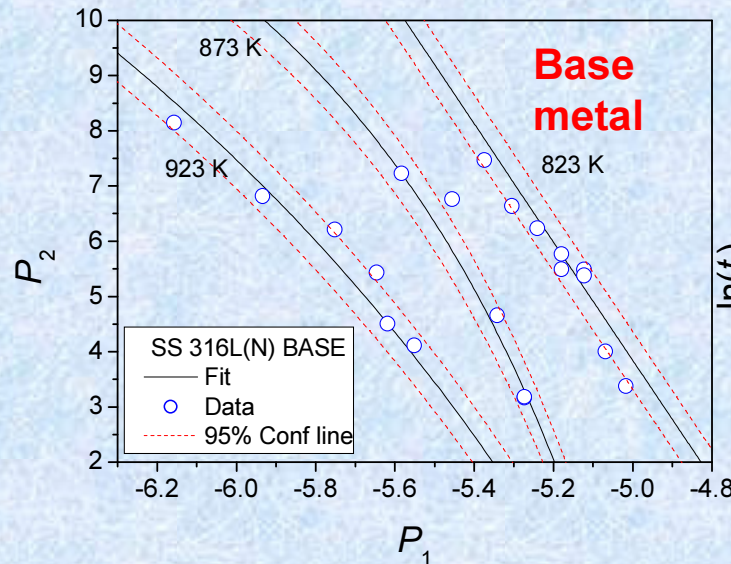
- Converts the *Information base* (multi-heat rupture data) to *knowledge base*
- Uses two heat indexing constants



Literature Data on SS 316 & SS 316L(N)
+ RSR Heat indexing Method
→ Knowledge base

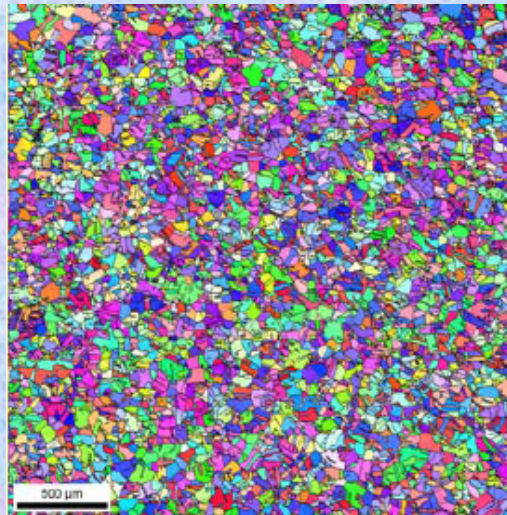
$P_1 \equiv \ln(\sigma/\mu) + \beta_k$; $P_2 \equiv \ln t_r - \alpha_k$
Isothermal reference correlations with literature data on SS 316+SS 316L(N) used for rupture life extrapolation of PFBR materials including weld

Use for rupture life extrapolation of base and weld materials of a new heat of SS 316L(N) (PFBR) demonstrated





Grain boundary engineering in austenitic stainless steel



Alloy A: Intermediate warm working temp., annealing during rolling process

→ uniform grain size

Minimum Time for sensitisation :

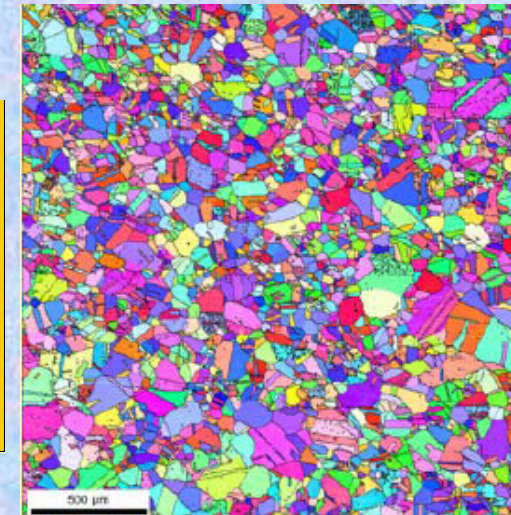
about 200 h

Alloy B: No intermediate warm working temp., annealing during rolling process

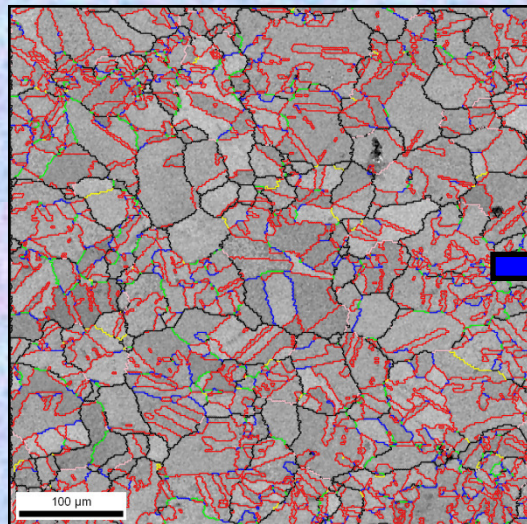
→ non-uniform grain size

Minimum Time for sensitisation :

more than 2000 h

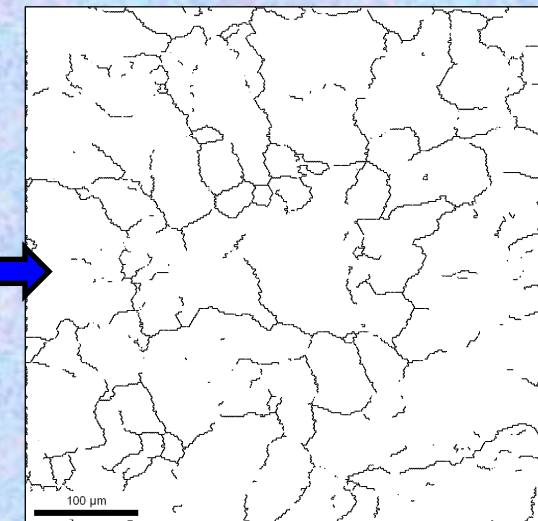


Grain boundary engineering in 316 L(N) to minimize sensitization



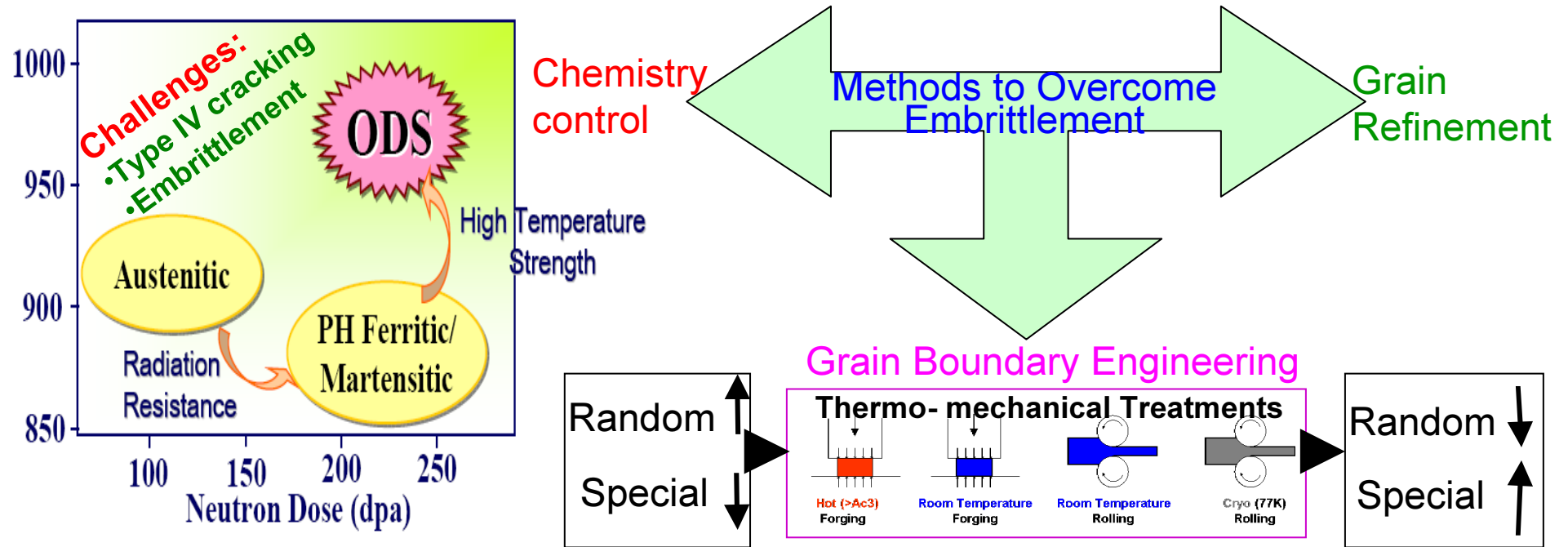
High fraction (80%) of CSL boundary achieved by thermo-mechanical processing to alleviate **Radiation induced segregation**

The high angle grain boundary map shows substantial disruption in random high angle boundary connectivity due to high fraction of CSL **No percolation**



Grain boundary engineering in alloy D9 to minimize radiation induced segregation

Ferritic Steels for Future Fast Reactor Core



Progress So Far:

- Prediction by Monte Carlo Methods and Percolation Model \Rightarrow 80% special boundaries
- Identified the Thermo-mechanical Treatment to decrease Effective Grain Boundary Energy by 50%
- Increase in Room Temperature Absorbed Energy by 50 Joules by Grain Refinement
- Ductile to Brittle Transition Temperature decrease by about 20° by Grain Refinement



Resistance to Intergranular Cracking by Grain Refinement

Experimental confirmation in 9Cr-1Mo steel

Design of two step heat treatment

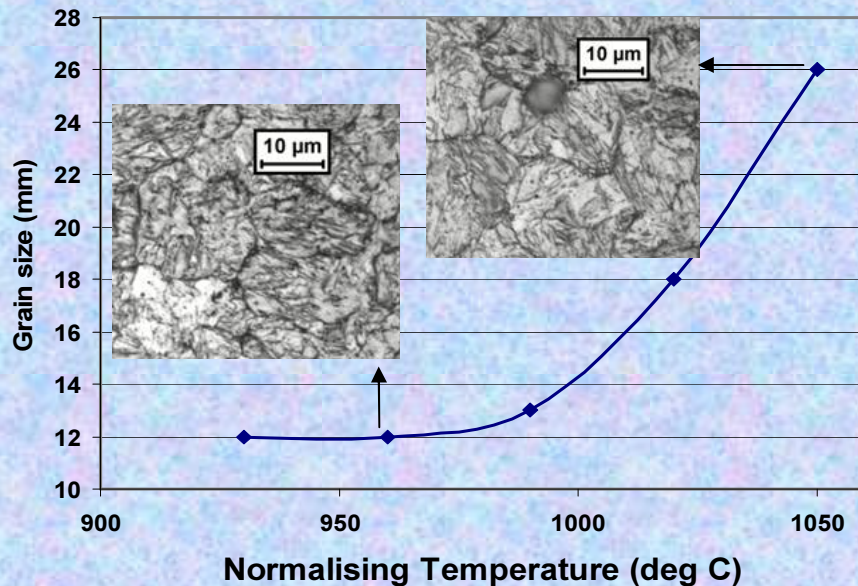


50% grain size refinement



Increase in Absorbed Energy

50 Joules



$$DBTT \propto (\text{grain size})^{1/2}$$

Geometric model using Monte Carlo

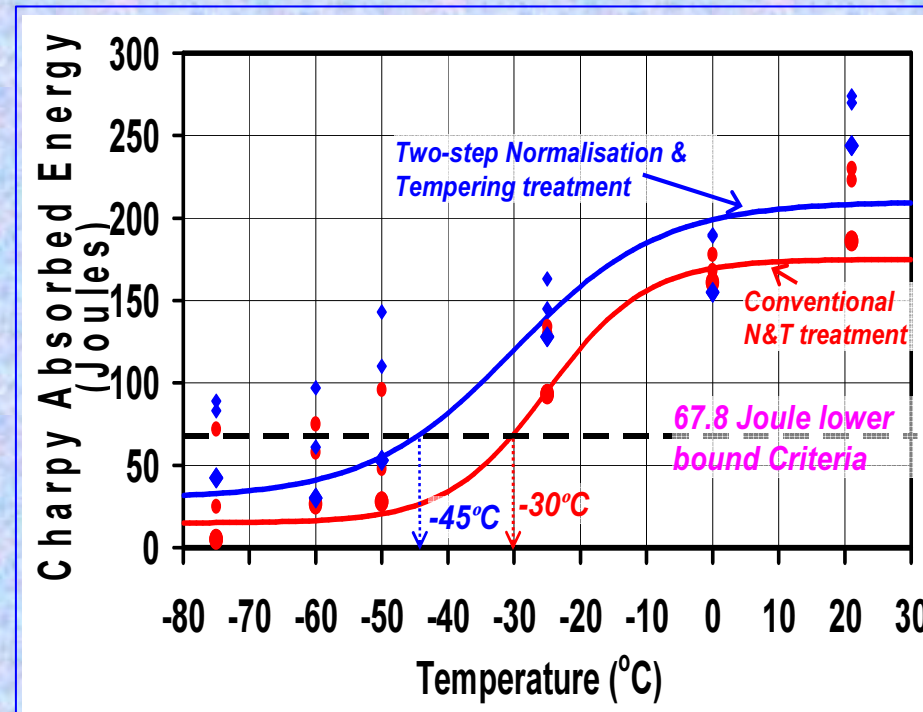
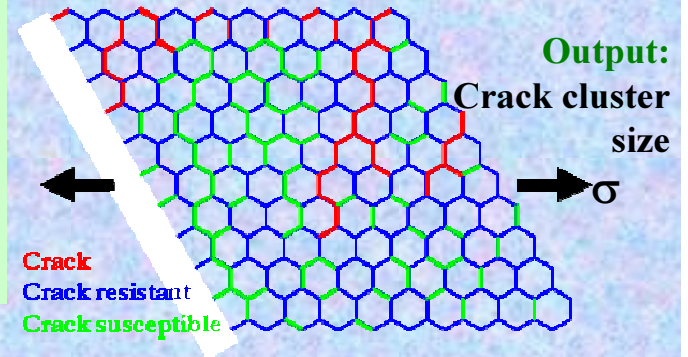
Inputs:

Array size: $n \times n$

MC cycles: M

weak boundaries frac.: f ,

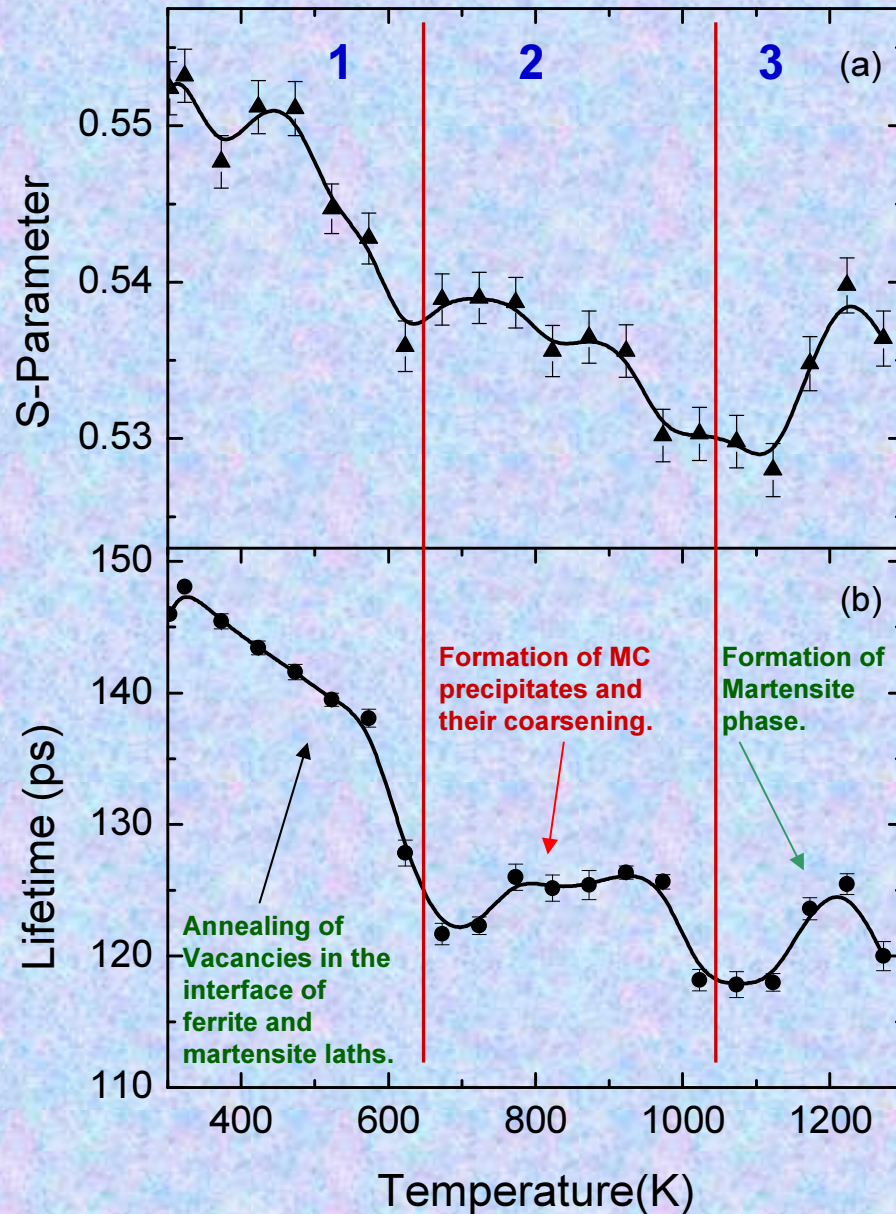
Avg. g.s.



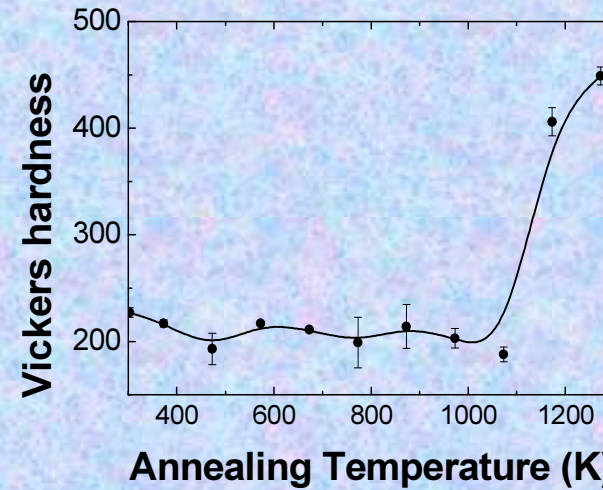
Grain refinement is beneficial in reducing embrittlement



Positron Annihilation Studies on Reduced Activation Ferritic/Martensitic Steel – Eurofer97



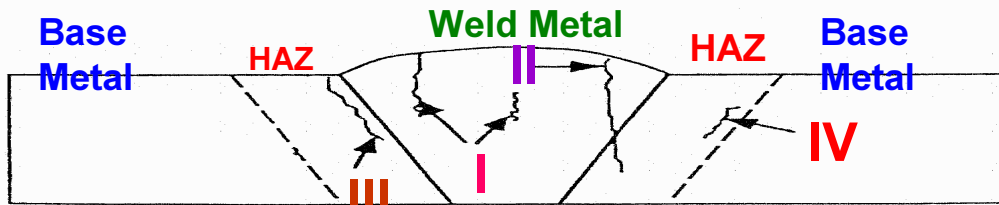
Clear changes are seen in lifetime and S-parameter at lower temperatures upto 470 K not seen by macroscopic techniques.



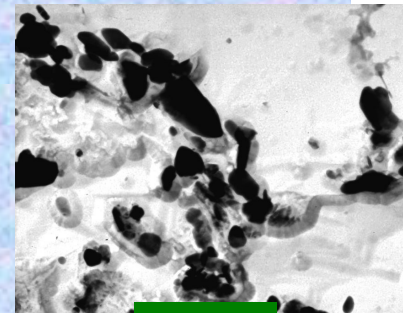
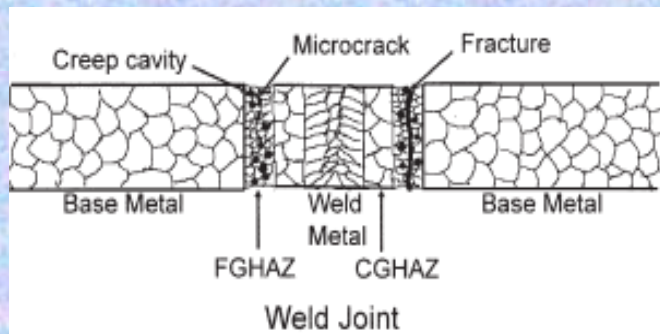
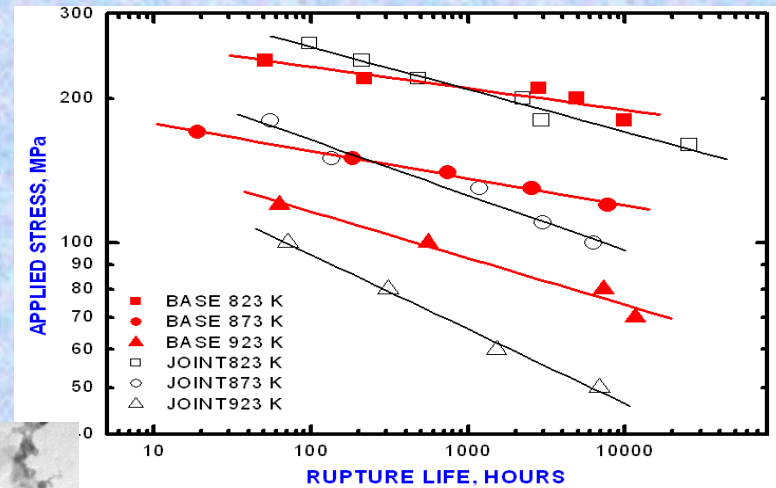
Hardness shows no signature of variation upto 1000 K, which is also supported by stable microstructure observed by microscopy. However, atomistic changes due to defect annealing and pre-precipitation can be studied using PAS.



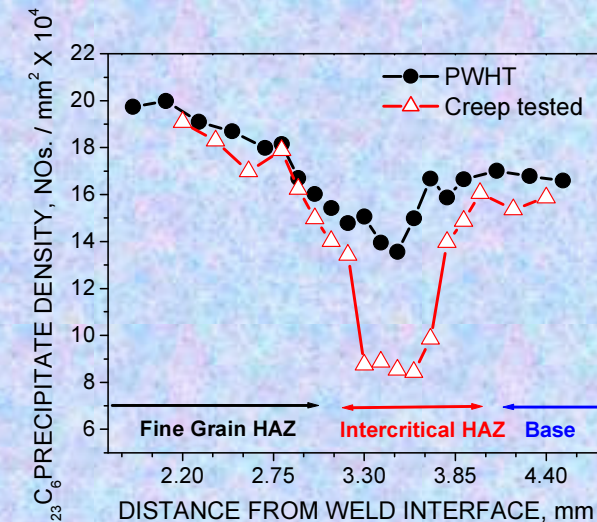
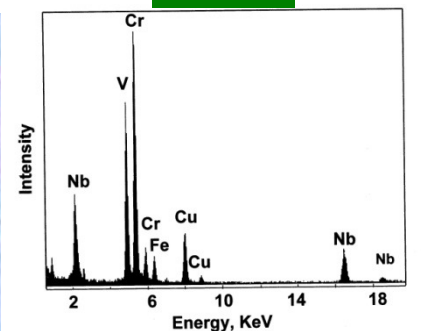
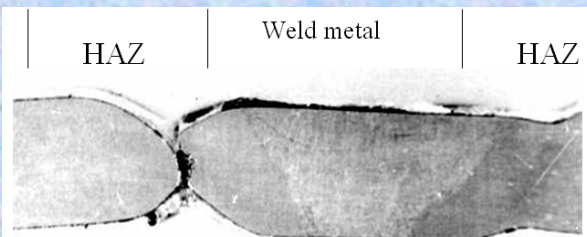
TYPE IV CRACKING IN INTERCRITICAL HEAT AFFECTED ZONE OF MOD. 9Cr-1Mo FERRITIC STEEL



- Type I - Cracking in Weld metal
- Type II - Crack initiated in weld metal propagated to coarse grain HAZ
- Type III - Cracking in coarse grain HAZ
- Type IV - Cracking in intercritical / Fine grain HAZ



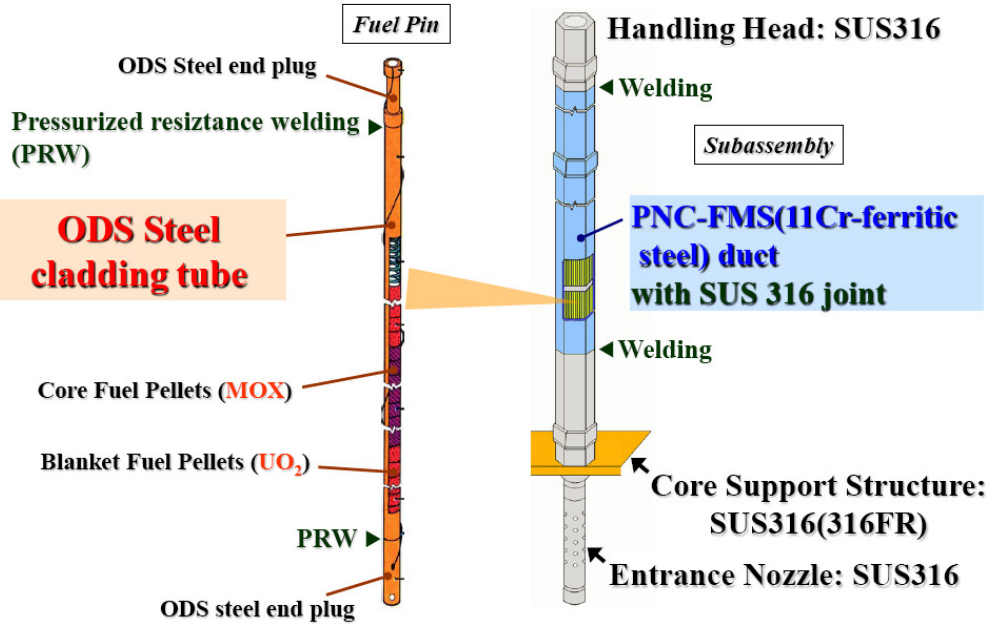
Z-Phase



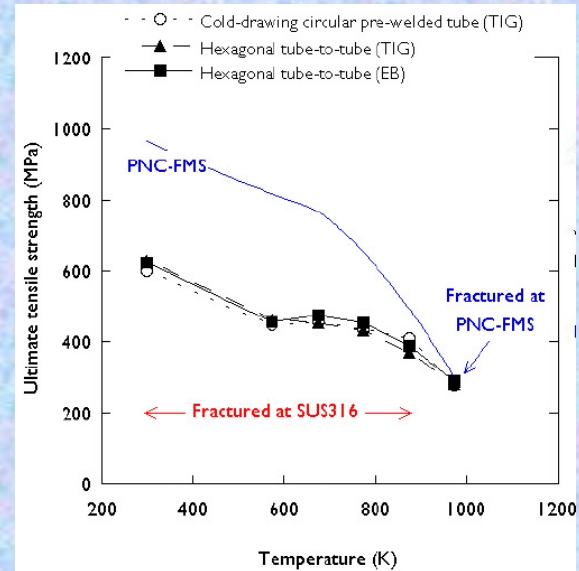
Coarse $M_{23}C_6$ and lower density in intercritical HAZ

BETTER DESIGN OF WELD, IMPROVED WELDING PROCESS AND ADDITION OF BORON AIDED IN THE DESIGN OF FERRITIC STEELS FOR TYPE IV CRACKING RESISTANCE

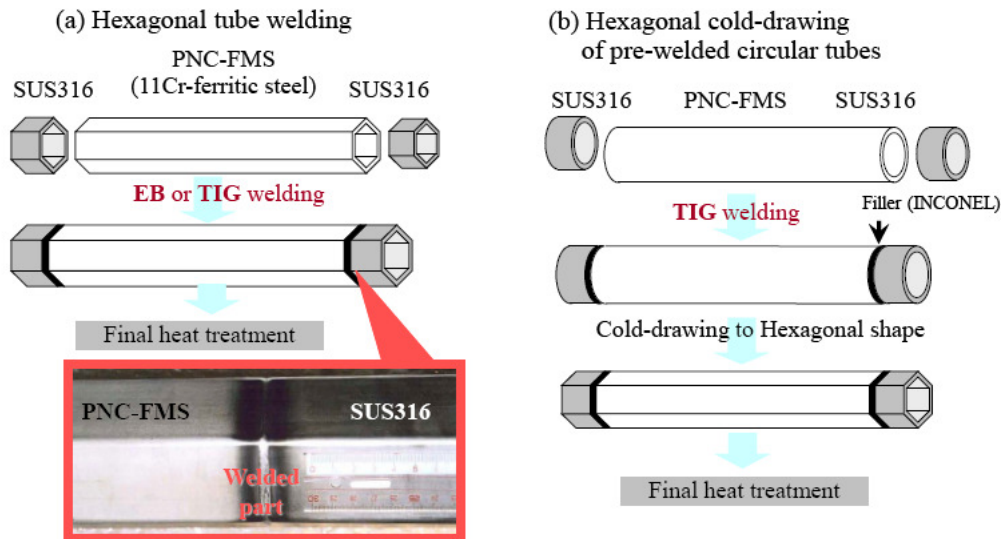
Basic structure of fuel pin and subassembly in JSFR



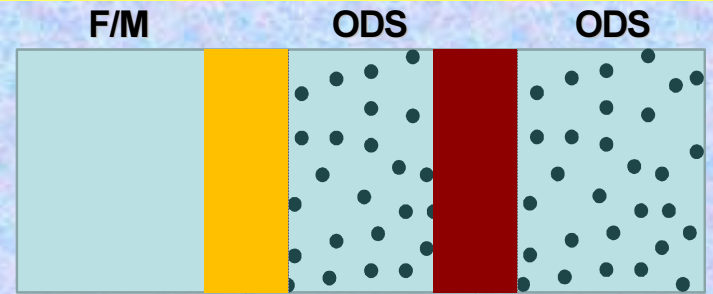
Weld and Joining Technologies under Investigation



PNC-FMS duct with SUS 316 short joint



Adequate strength at FMS/316 interface



- Fusion Welding**
- TIG (filler wire)
 - EB (without filler)

- Solid State Welding**
- Diffusion
 - Explosive
 - EMP
 - Friction Stir

GETMAT Approach

✓ Adequate strength at the FMS/316 dissimilar-welded part has already been proved by high-temp. tensile test in both case.



TRIMETALLIC TRANSITION METAL JOINT

316L(N) SS
[$\alpha = 18.5$]

ER 16-8-2
[17.3]

Alloy 800
[17.1]

Inconel 182
[15.5]

Mod. 9Cr-1Mo
[12.6]

• Improved Trimetallic Transition Metal Joint (TMJ) Configuration

Austenitic SS/Alloy 800/Cr-Mo steel trimetallic TMJ

16-8-2 consumable for Austenitic SS/Alloy 800 joint

• **Optimum Post Weld Heat Treatment**

– 1023 K (1 hr) for Mod. 9Cr-1Mo steel/Alloy 800 joint

• **4-fold improvement in service life**

– Compared to bimetallic joints

• Benefits

– Gradual transition in α ($\mu\text{m}/\text{m}/\text{K}$) across the joint

• **Reduces stress concentration**

– Hoop stress at Cr-Mo steel/ Inconel 182 WM interface

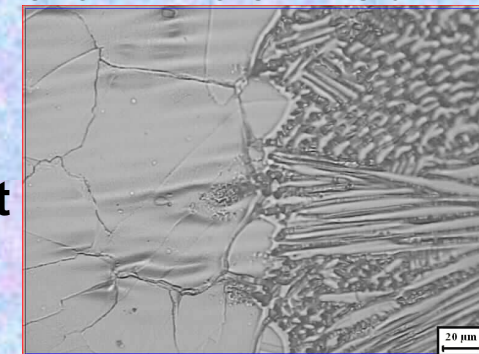
• **Decreases by 37%**

– Alloy 800

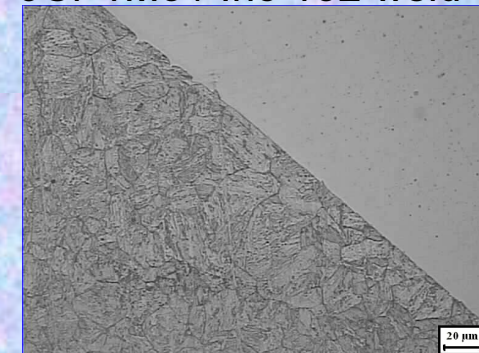
• **At elevated temperatures**

– **Excellent resistance to Oxidation & Creep**

316LN / 16-8-2 weld



9Cr-1Mo / Inc-182 weld




Experience gained from trimetallic joint technology developed for PFBR steam generators would be used for core subassemblies



Path of the development of material strength standard

To develop material strength standard for JSFR

(1) Extension of design life




The design life of DFBR is 60 years (approximately 530,000 hours).

The longest allowable limits of DDS is 300,000 hours

([DDS-Demonstration reactor Design Standard](#))

The extension of the longest allowable limits is necessary


(2) Applicability of various products



DFBR needs various products such as large diameter forged ring and small diameter thin walled tube and so on

Whether the allowable limits of DDS can be applied to such shape of structural material should be confirmed

(3) Allowable stress for welded joints



Especially for modified 9Cr-1Mo steel, creep strength degradation is observed in welded joints (“Type-IV” damage).

For the determination of allowable stress, “Type-IV” damage must be taken into account.

Modelling of mechanical properties of 9Cr-1Mo steel

The characteristic of DDS (1/2)

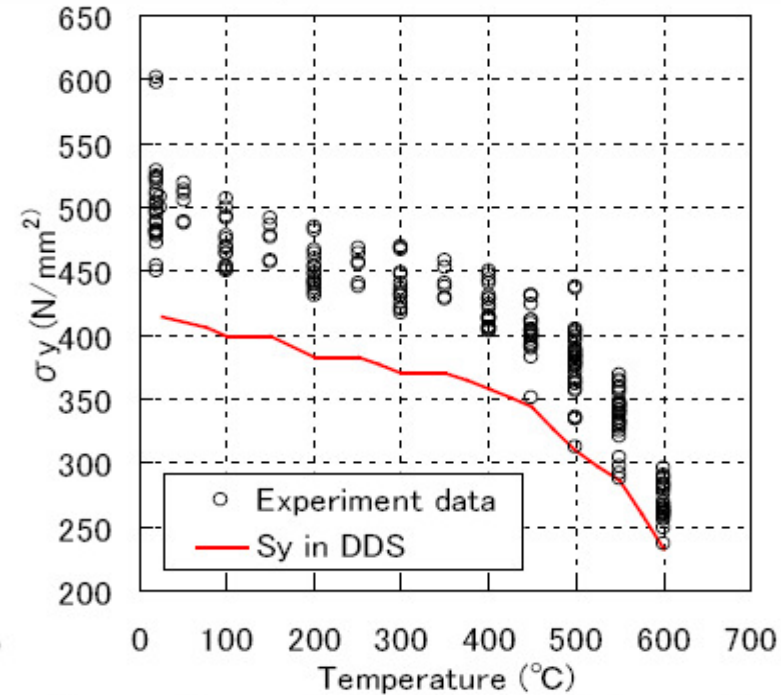
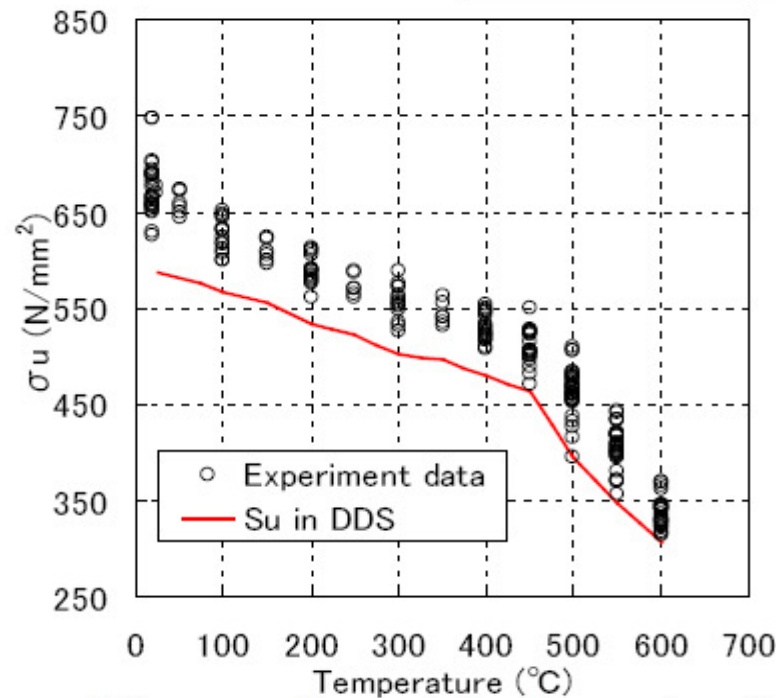
Mod.9Cr-1Mo

Formulation method of

σ_u (Design tensile strength),

σ_y (Design yield stress)

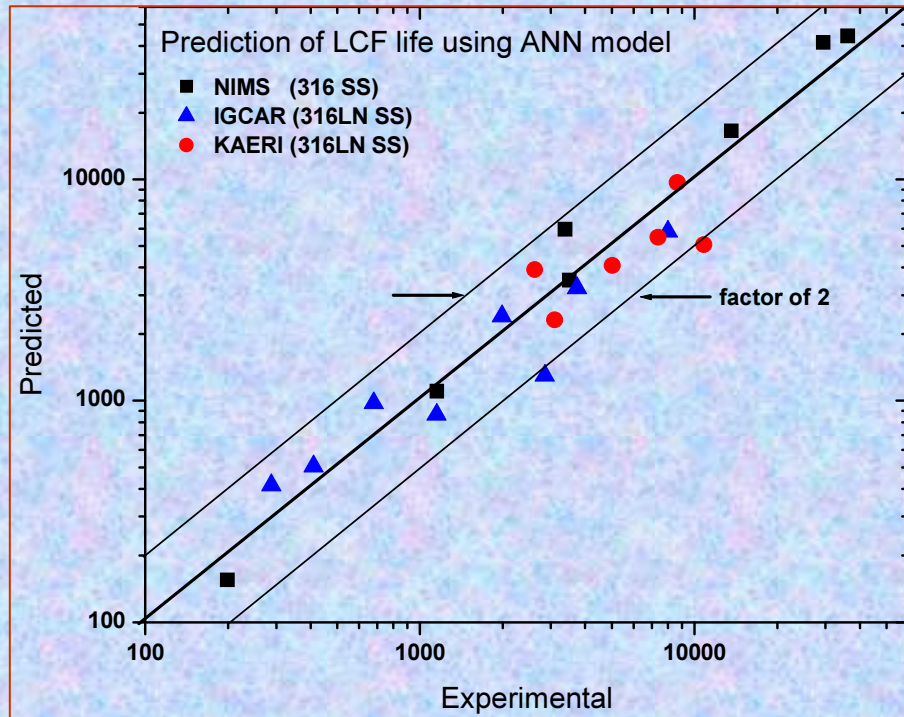
| | Number of heat | Temperature(°C) | Number of data |
|---------------|----------------|-----------------|----------------|
| Plate | 7 | RT~600 | 124 |
| Forging | 2 | RT~600 | 62 |
| Thick Forging | 3 | RT~600 | 52 |



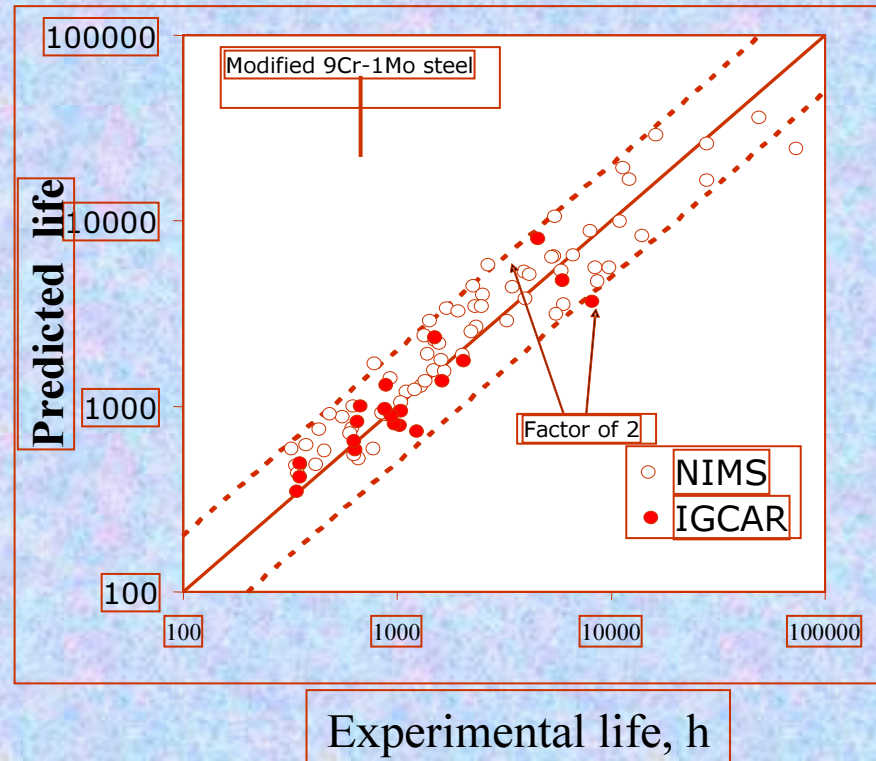
σ_u and σ_y were formulated based on the lower bound of 99% confidence level against tensile strength and yield stress (0.2% proof strength)
(Room temperature value is same as Gr.91 of ASME)



Fatigue Life Prediction Approaches



Prediction of LCF life of 316LN Stainless Steel using Artificial Neural Network (ANN) model



Life prediction using Ostergren's frequency modified damage function approach that uses the net tensile hysteresis energy to predict the cyclic life)

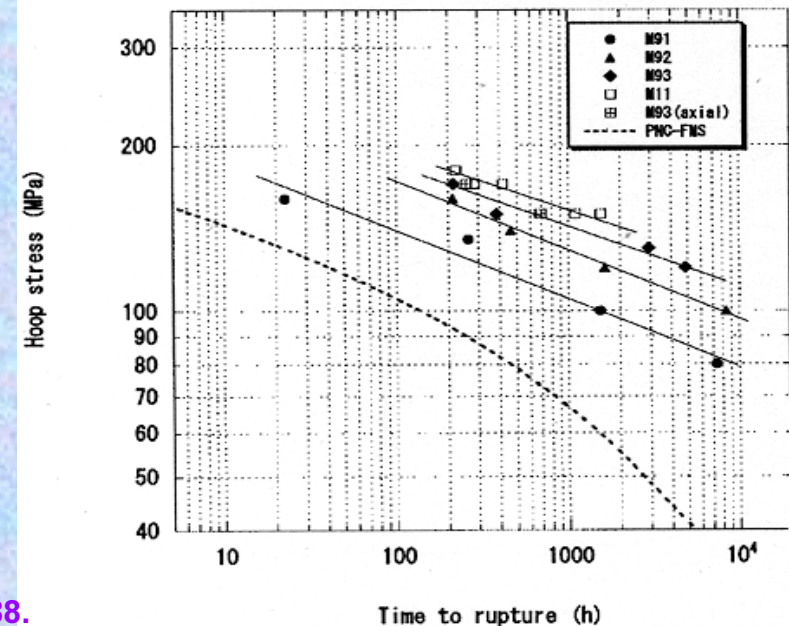
Extrapolation of laboratory data to design conditions using numerical and mechanistic approaches.

Oxide Dispersion Strengthened (ODS) Alloys

- Ferritic structure provides better resistance to neutron damage and has better void swelling resistance. (Compared to austenitics)
- **DBTT is close to room temperature**
- **No carbon leaching in sodium environment**

Creep strength increases with increasing Ti content from 0.1(M91) to 0.2 (M93) wt% and Y_2O_3 from 0.30 (M92) to 0.37 (M11) wt%

S. Ukai, et al J. Nuclear Science and Technology, 2002, Vol. 39, 778-788.



➤ Better creep strength at high temperature than ferritic steels due to high density of highly stable nano clusters – produced by mechanical alloying which reduce creep rate by 6 orders of magnitude at 650–700°C

• These clusters are self assembled after high temperature treatment of mechanical alloy powders and ultrastable. (No coarsening after 14000 hr creep studies at 800°C, contrary to other nanophase materials with rapid coarsening at high temperature)

• Basic issue is to understand the role of defects, i.e., vacancies produced by mechanical alloying and Ti in the stability and structure of the nano clusters. Explore possibility of other elements eg Zr.

- **Production of ODS alloys requires strict control over powder purity to avoid creep crack initiation at prior particle boundaries in HIPed products.**
- **Development of suitable joining technologies.**

Alloy design and phases for candidate ODS Steels

| mass% | C | Cr | W | Ti | Y ₂ O ₃ | Excess O |
|----------|------|------|-----|------|-------------------------------|----------|
| | M | M | S | D | D | D |
| 9Cr-ODS | 0.13 | 9.0 | 2.0 | 0.20 | 0.35 | 0.07 |
| 12Cr-ODS | 0.03 | 12.0 | 2.0 | 0.26 | 0.23 | 0.07 |

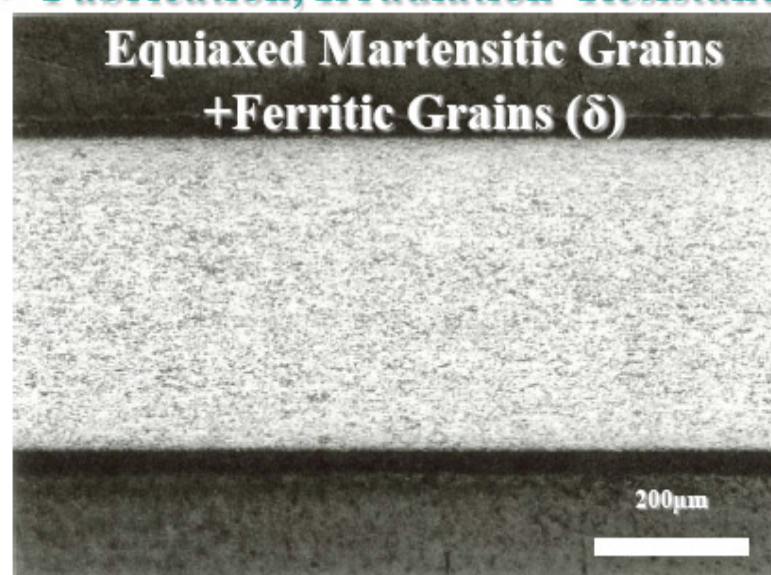
M: Phase Control
S: Solution Hardening
D: Dispersion Hardening

Oxygen in Y₂O₃ = Excess Oxygen

Primary Candidate

9Cr-Martensitic

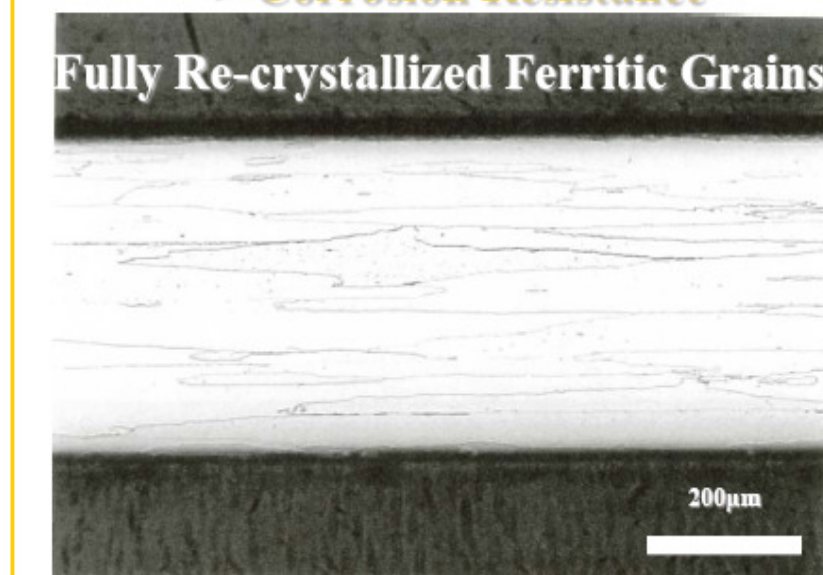
=> Fabrication, Irradiation Resistance



Secondary Candidate

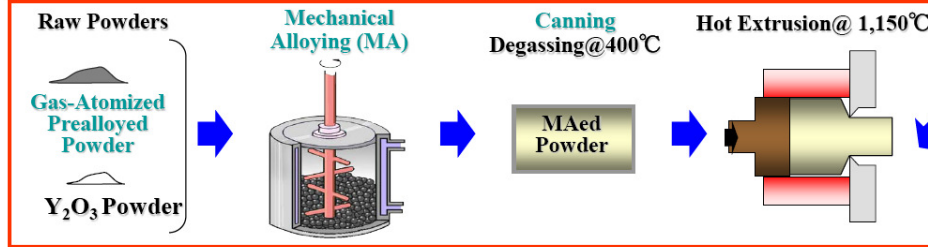
12Cr-Fully Ferritic

=> Corrosion Resistance

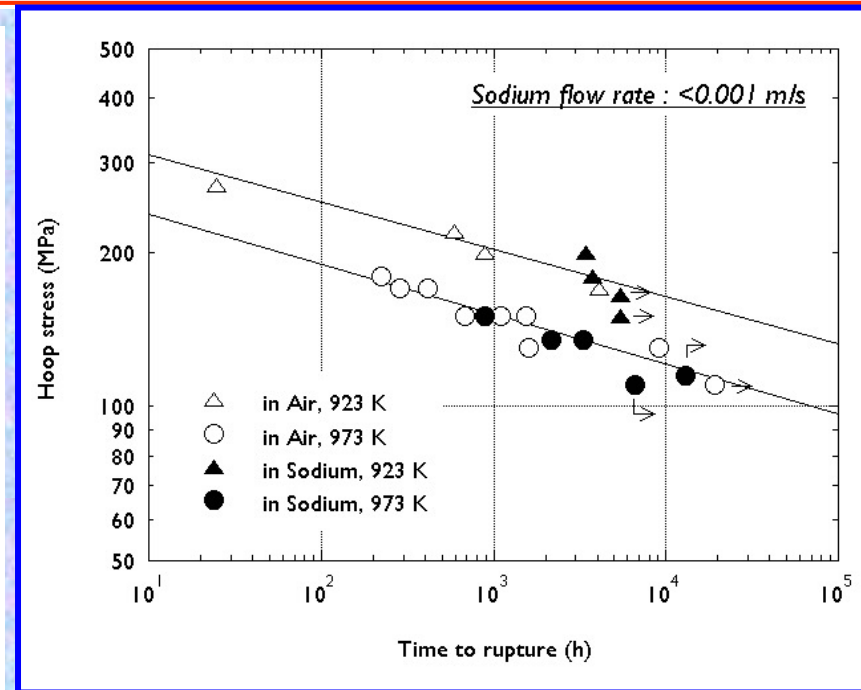
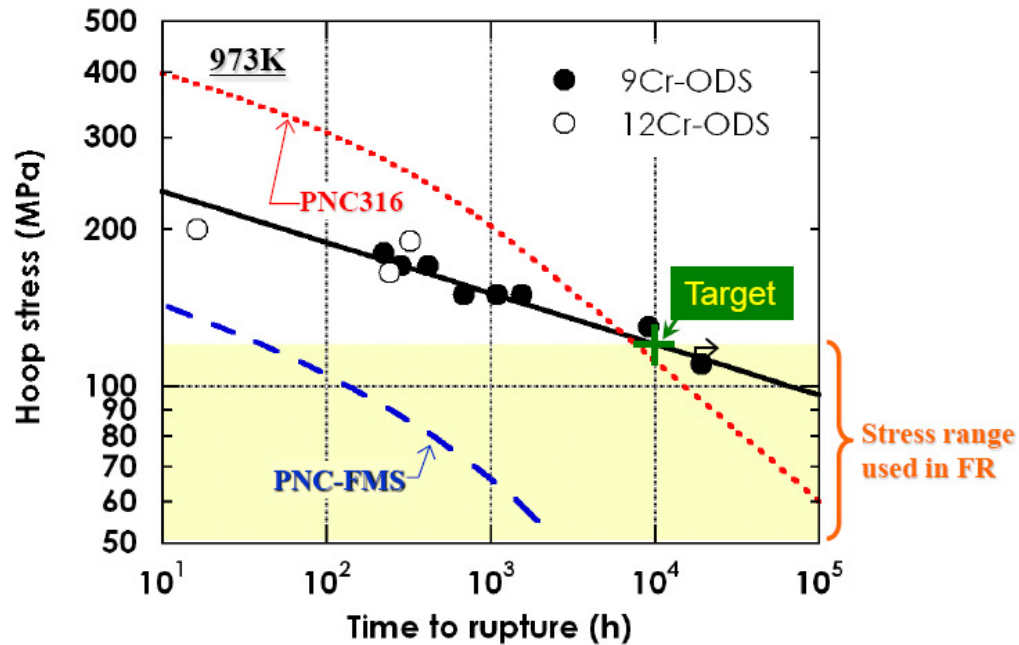
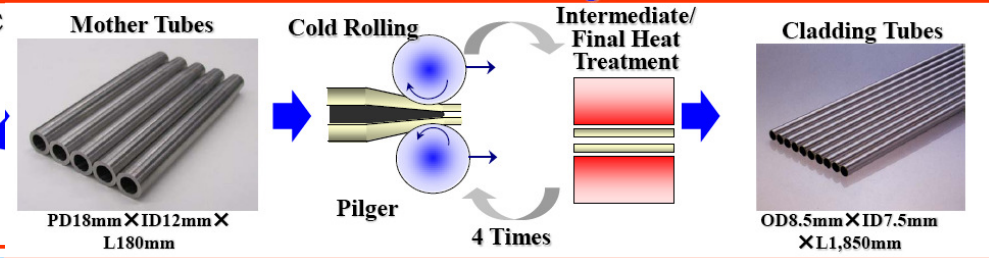


Manufacturing process and Out-of-pile creep rupture properties of ODS Steel

Powder Metallurgy Process



Thin Wall Precise Tubing Process



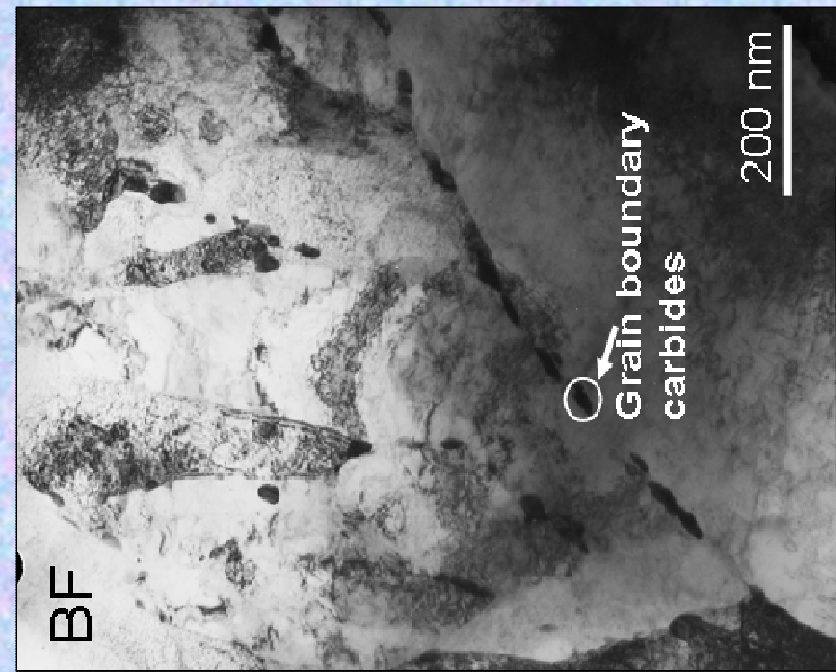
JAEA developed high-strength ODS steel tube, which achieves the target out-of-pile creep strength of 120 MPa for 10,000 h at 973 K



9Cr-ODS Cladding Tubes (Normalized +Tempered) Manufactured in India



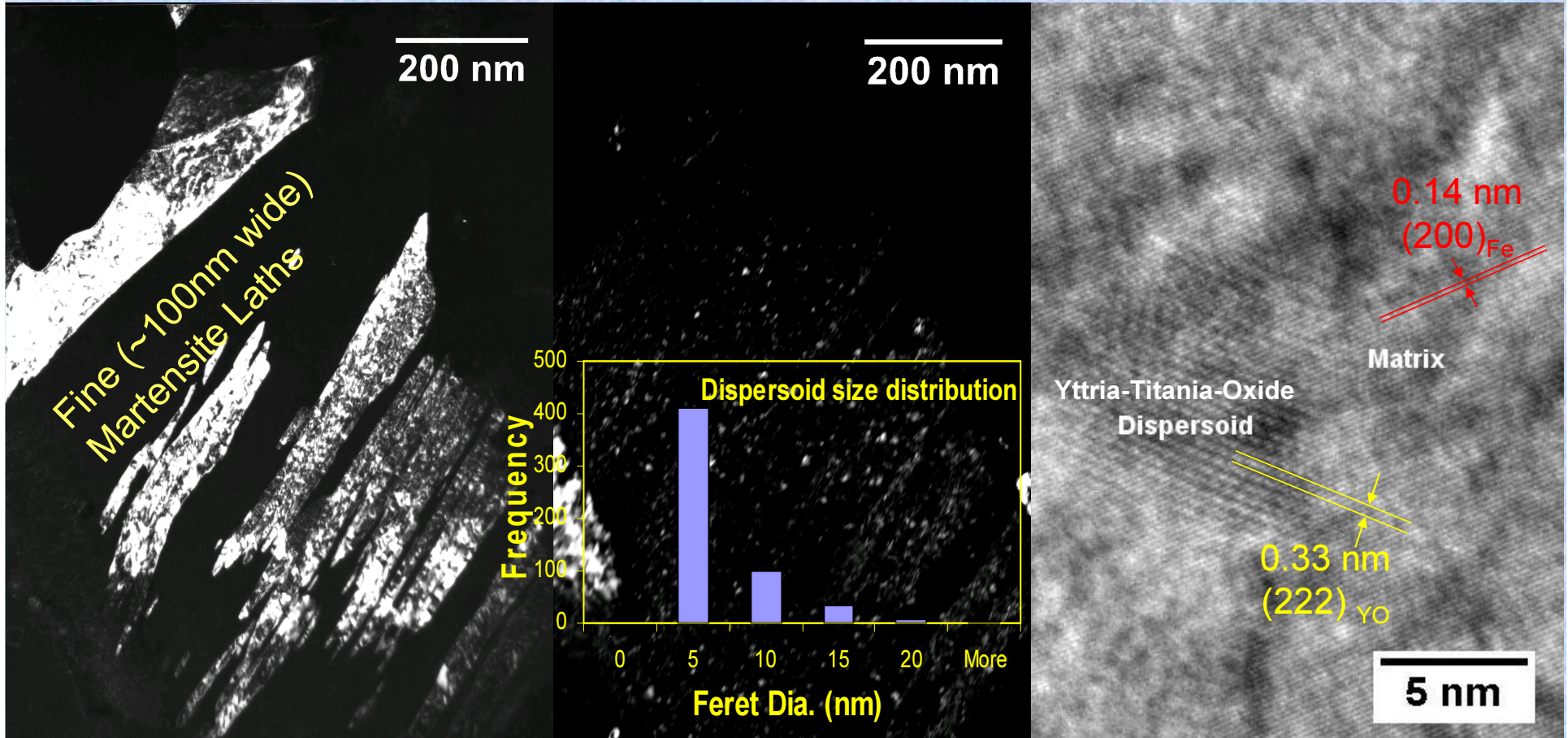
Clad tube (1.5 m) of 9Cr ODS ferritic-martensitic steel



Transmission electron micrograph showing a typical tempered martensitic structure with carbide precipitates decorating the lath and prior austenite grain boundaries



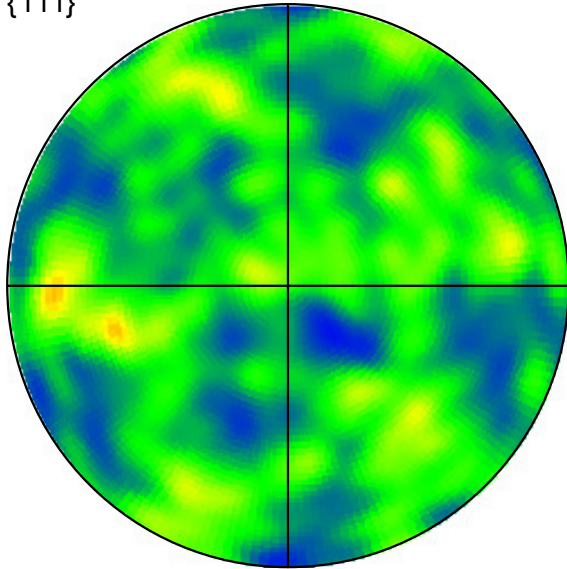
Microstructure of Fe-9Cr-0.11C-2W-0.2Ti-0.35Y₂O₃ ferritic-martensitic ODS alloy developed in India





Microstructure@ EBSD on Flattened Tube

{111}

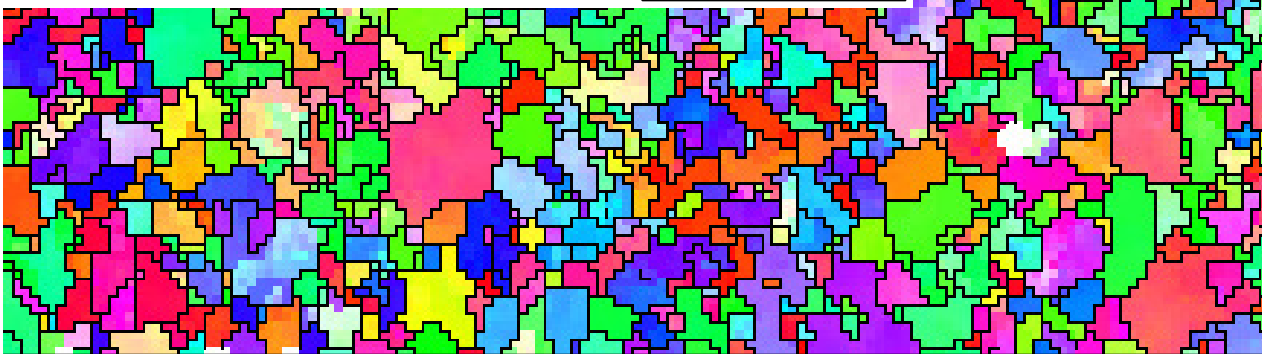
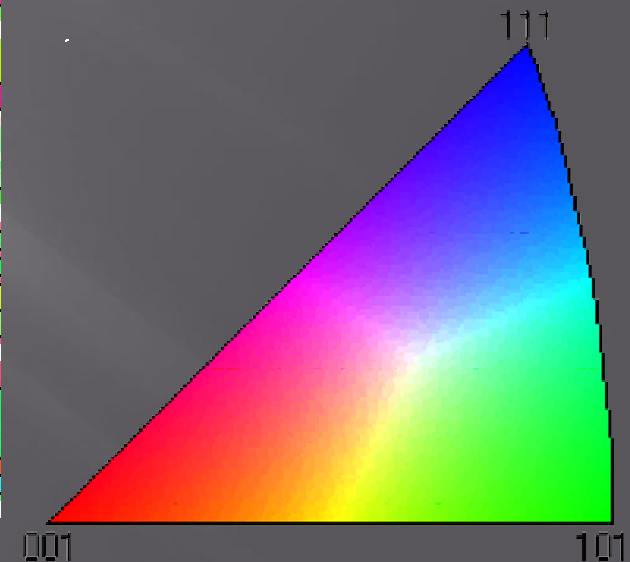
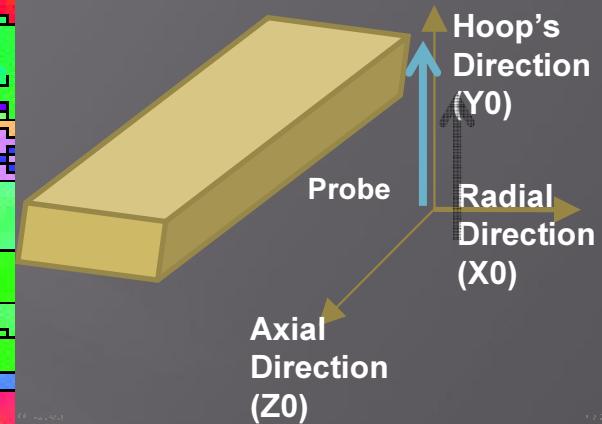
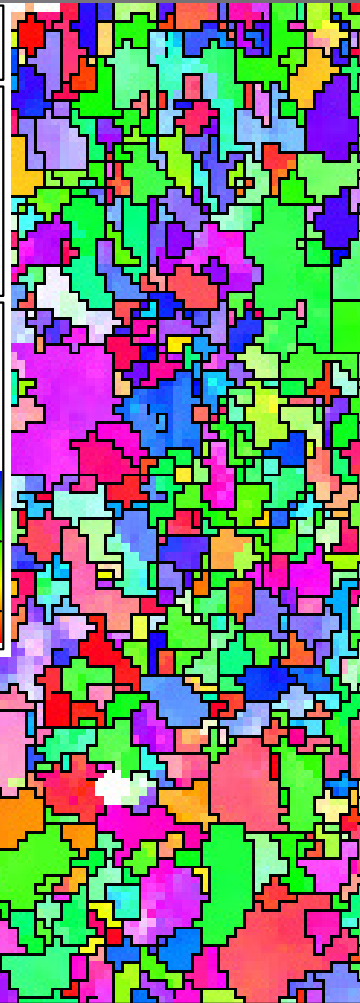
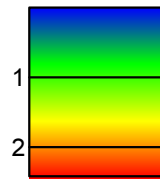



Pole Figures

[Project4.cpr]
Iron bcc (old) (m3m)
Complete data set
16737 data points
Equal Area projection
Upper hemispheres

Half width: 10°
Cluster size: 5°

Exp. densities (mud):
Min= 0.38, Max= 2.45



 = 20 μm ; IPF Coloured; Step=0.8 μm ; Grid 146x115

Grain size morphology showing reduced anisotropy in 9Cr-ODS due to intermediate heat treatments during cold rolling and final heat treatment

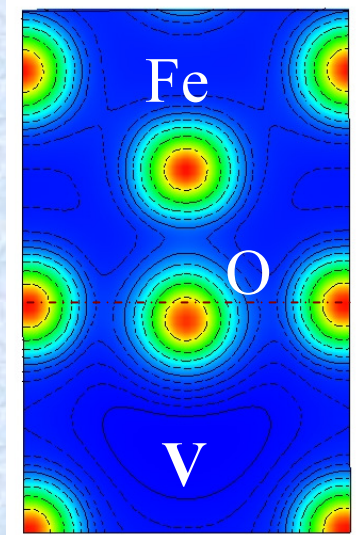
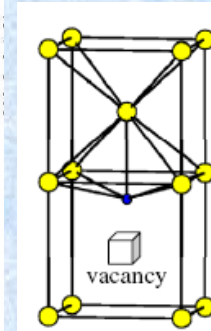
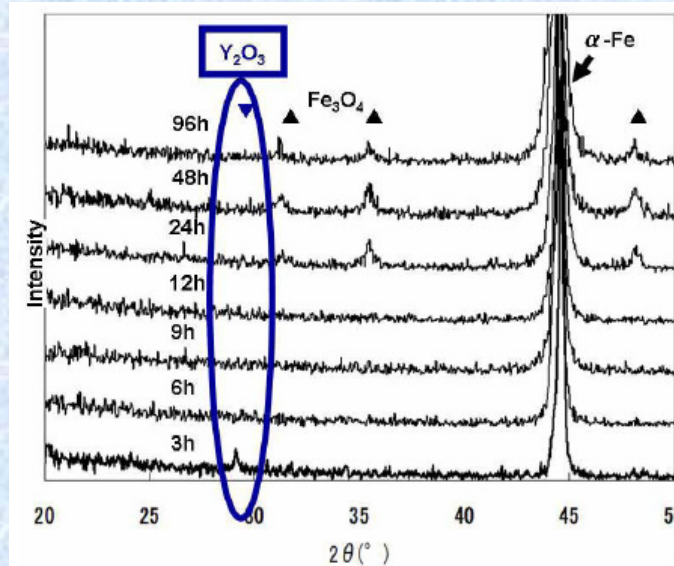
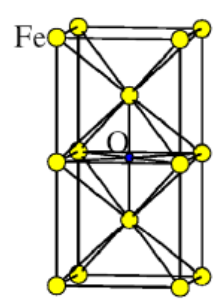
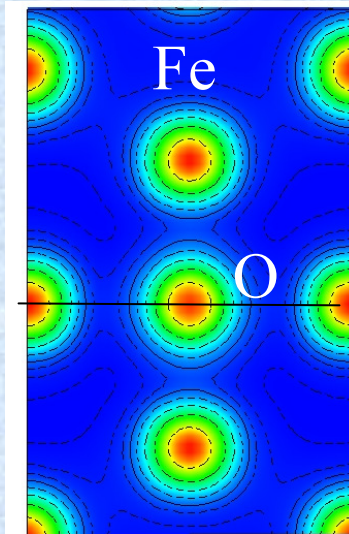


Formation and stability of O-enriched Ytria-Titania nano clusters in Fe - Ab-initio total energy calculations of defects in Fe

Enhancement of O solubility in Fe in presence of vacancy

Calculation using VASP abinitio code - 128 atom super cell

Oxygen peak vanishes as a function of Mechanical alloying



Charge density of octahedral oxygen in Fe in (110) plane

$$E_{f_O}^f = 1.35 \text{ eV}$$

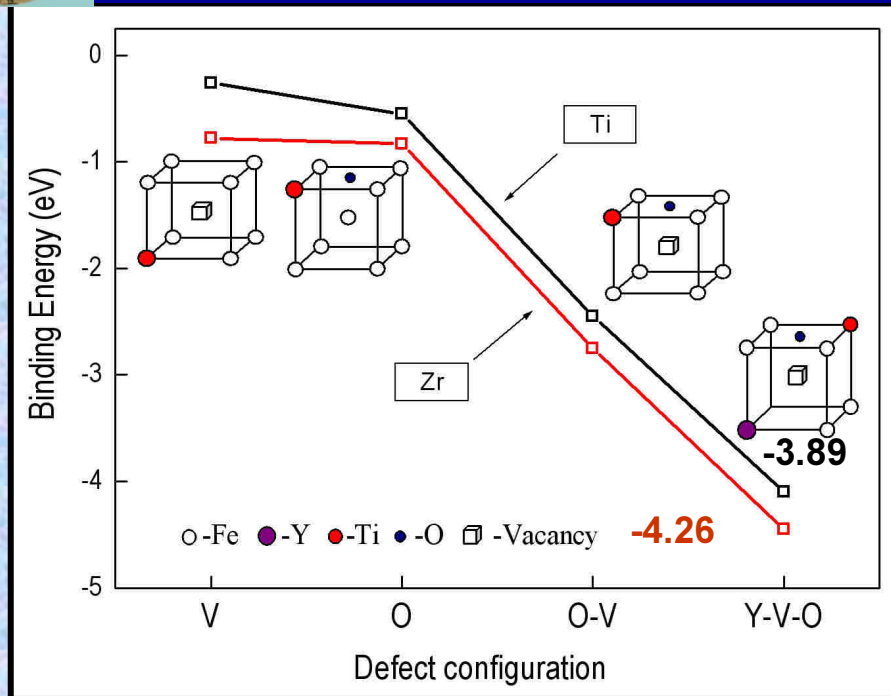
$$E_{f_{O-V}}^f \sim 0 \text{ eV}$$

Charge density in the (110) plane of octahedral oxygen with the presence of vacancy. O moves towards Vac by 0.2 Å

Vacancies introduced by Ball Milling increases solubility of Oxygen in Fe matrix and enables regrowth of Y-Ti-O particles with refined dispersion



Effect of Minor Alloying Elements-Ti and Zr on Yittria Dispersion



The binding energies of Ti and Zr atoms with vacancy(V), O, O-V, Y-V-O cluster in bcc Fe. The schematic of the atom positions also shown in the picture.

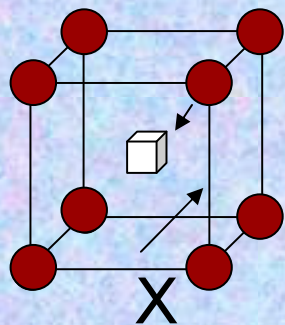
Calculation using VASP abinitio code - 128 atom super cell

Ab-initio density-functional theory binding energy calculations indicate that the binding energy of the defect clusters increases when Ti is replaced with Zr, which leads to finer dispersion of nanoclusters which could result in improved performance of ferritic alloys.

This prediction is consistent with the experimental results. [Uchida et al. Mater. Res. Soc. Symp. Proc. Vol. 981 © 2007 reported smaller nano clusters for Zr (10nm) as compared to Ti (15nm)]

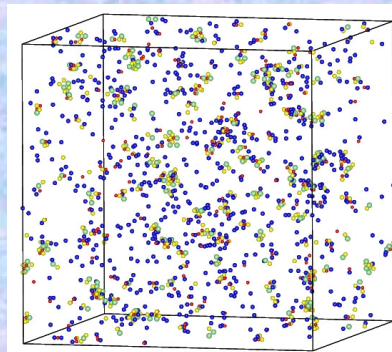


Lattice Kinetic Monte Carlo simulation of Y-Ti-O nanocluster formation in bcc Fe

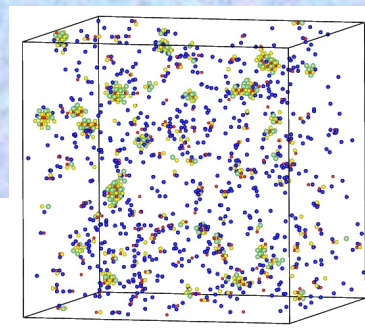


A: Fe, Y, Ti, V
B: O

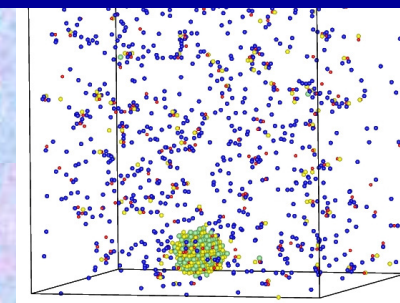
- Ti
- Y
- O
- V



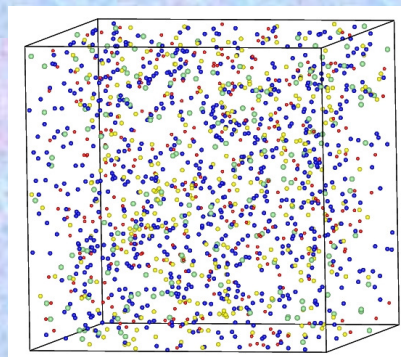
0.02 million MCS



0.1 million MCS

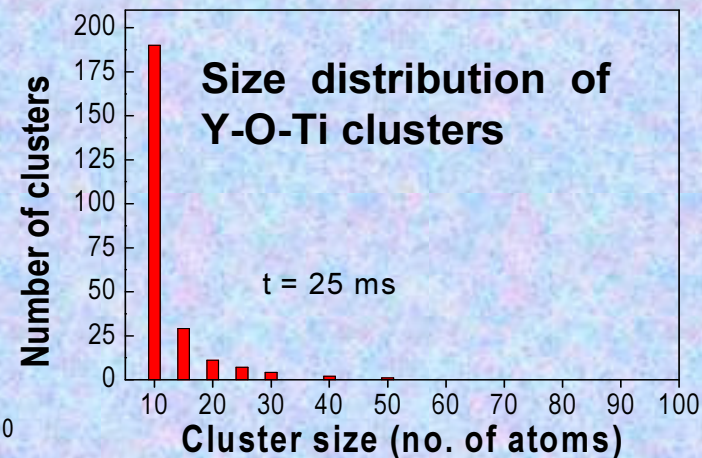
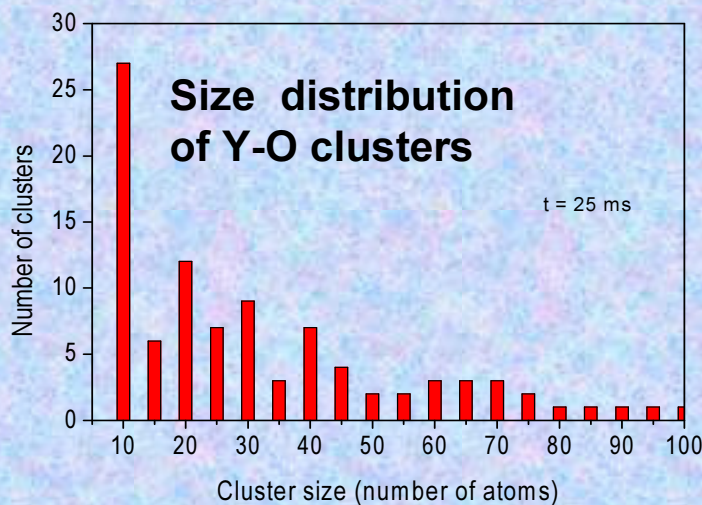


5 million MCS



Random distribution

**T = 877 °C ; 42x42x42
bcc Fe supercell ; Ti
– 0.5%, Y₂O₃ – 0.3%
Vac – 0.1%**

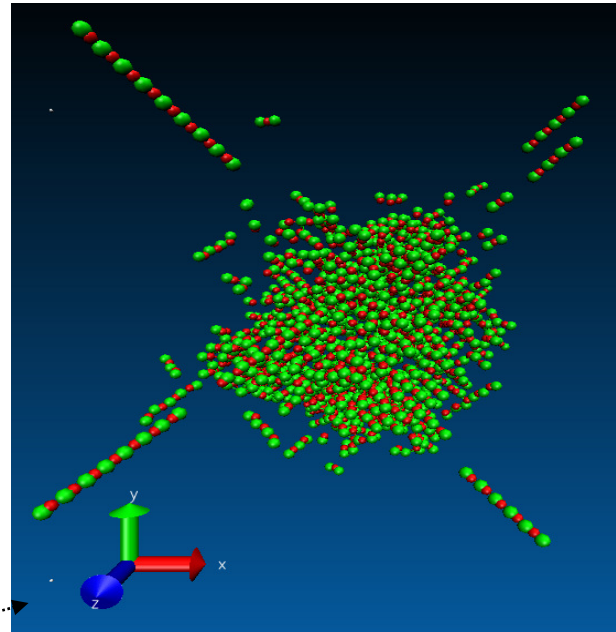
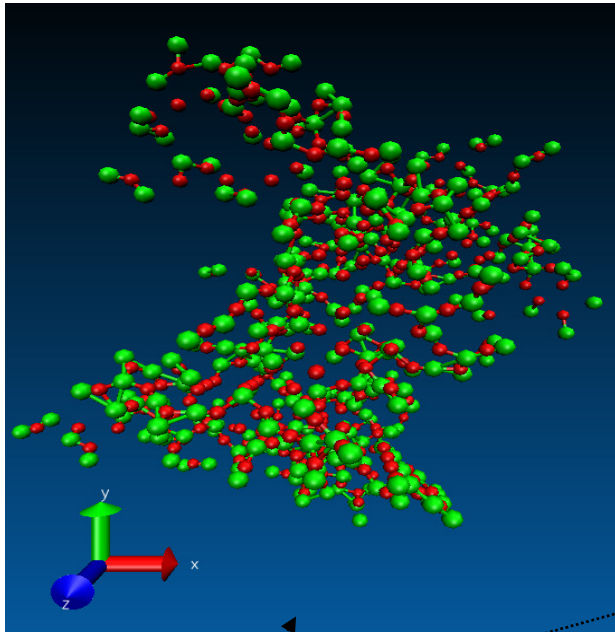


Refinement of nano cluster dispersion with Ti addition



Simulation of radiation damage cascade

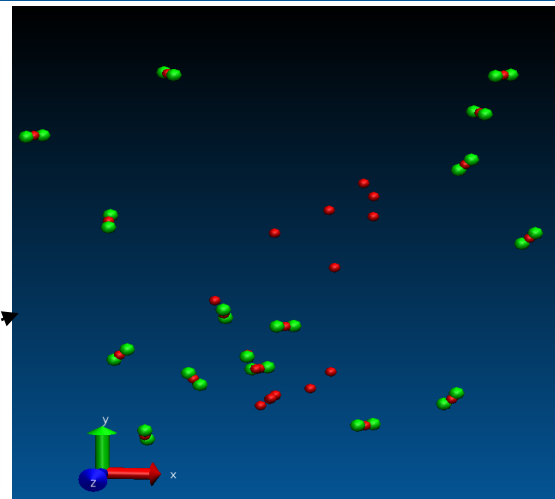
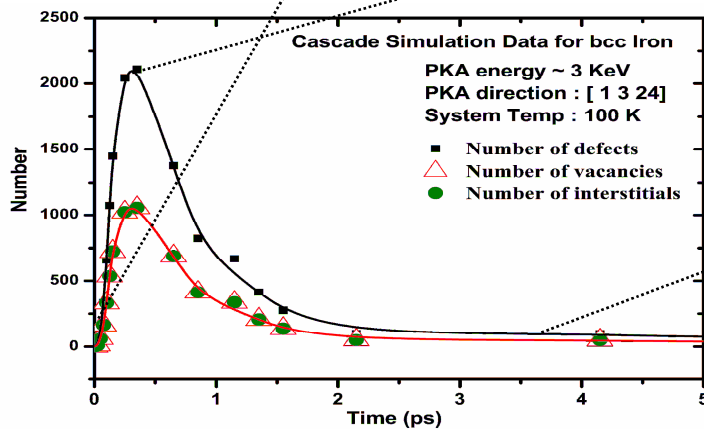
Damage cascade in *bcc*-Fe, 0.25 million particles, up to 50 ps.



Green balls: interstitials,
Red balls: vacancies.

Graph shows variations
in number of vacancies
and interstitials with time.

Regions indicated by
arrows correspond to
defects present at
initiation, in thermal
spike regime, and after
annealing stage.

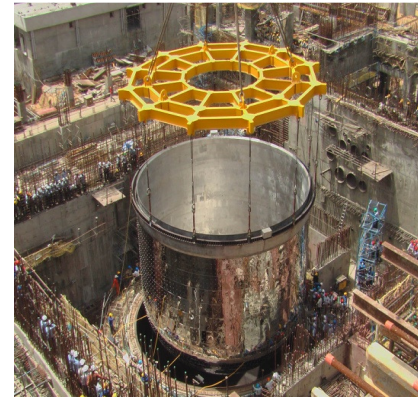


dumbbell structures
comprising of 2
interstitials and single
vacancy are stable.



Manufacturing of large components of PFBR with close tolerance

- Achieving high manufacturing tolerances for thin walled large diameter vessels better than those achieved internationally
- Precise machining tolerances for grid plate
- Innovative methods of handling vessels without welding
- Consistency with the specified erection tolerances



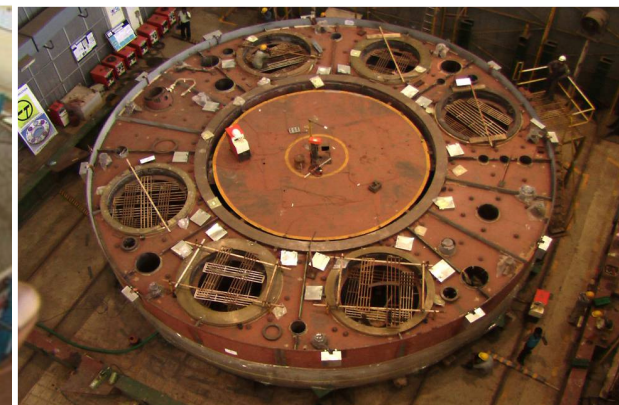
Erection of safety vessel in June 2009



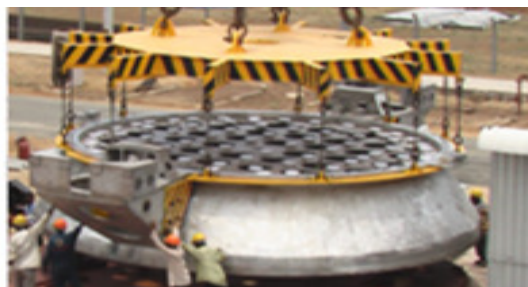
Grid plate with primary pipes



Inner vessel



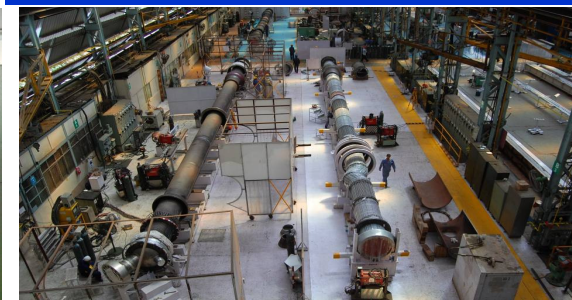
Roof slab



Core support structure



Primary sodium pump



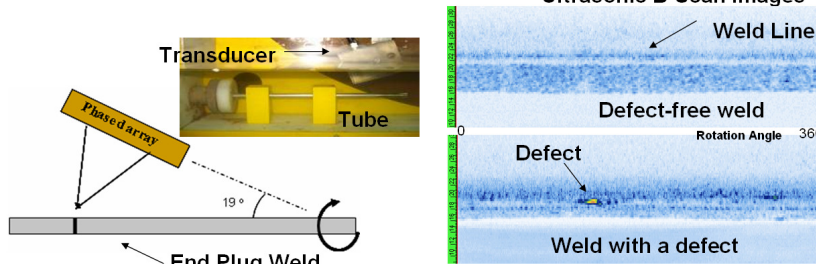
Steam generator



Non Destructive Evaluation & Inspection Technologies

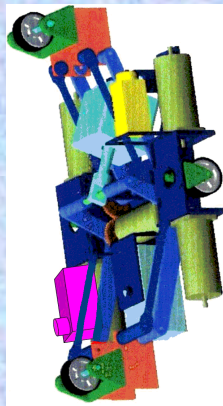
- Tight discontinuity with shorter circumferential extent – lack of fusion/ lack of penetration
 - Extent of coverage
- Detection sensitivity for phased array UT – 100µm dia and 150µm deep hole in weld

High Frequency (17 MHz) 128 element linear phased array immersion probe employed

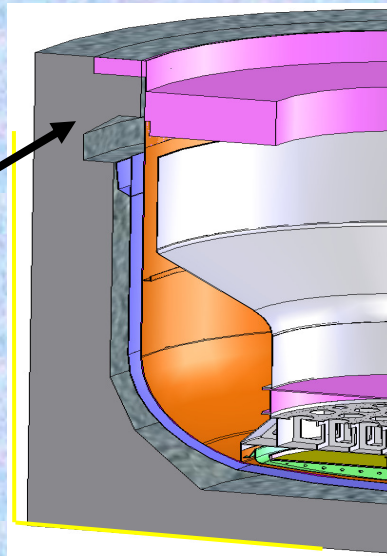


Phased Array UT enhances the reliability compared to radiography

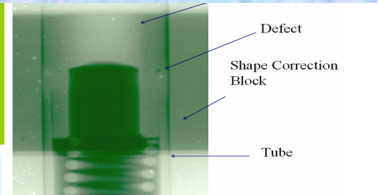
Inspection of fuel pin end plug



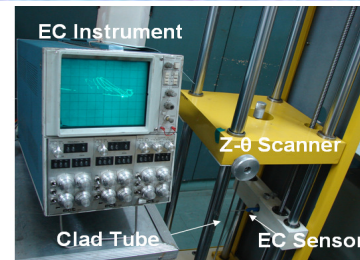
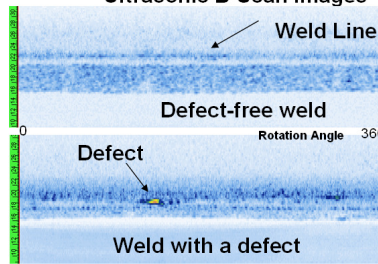
ISI of bimetallic (SS & CS) weld



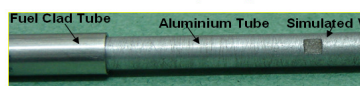
In-service Inspection of Main Vessel



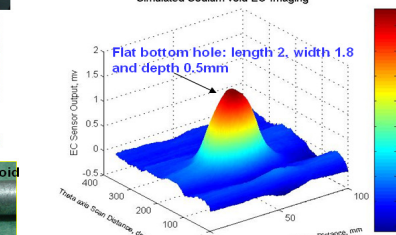
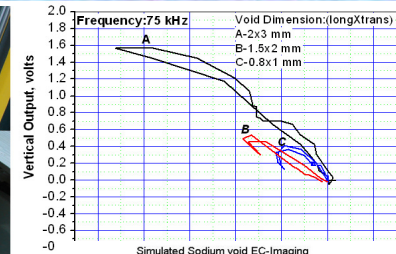
Ultrasonic B-Scan Images



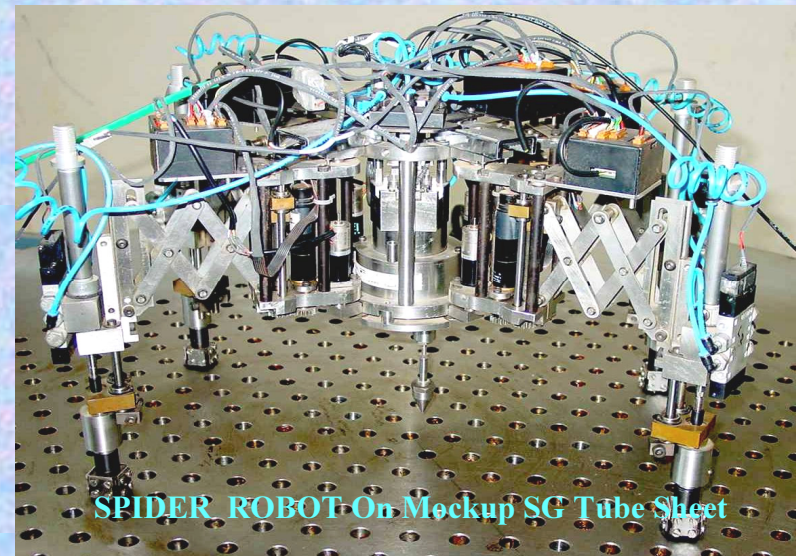
Voids in Sodium encapsulated between Quartz (outer) and SS tube



Simulated Void in Al tube (equivalent conductivity)



Eddy Current Imaging Technique for Detection of Voids in Sodium Bonded Metallic Fuel Pins

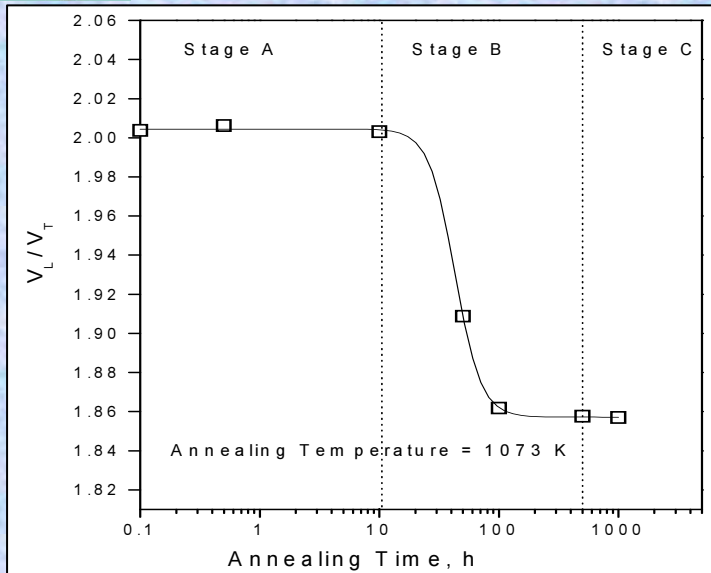


SPIDER ROBOT On Mockup SG Tube Sheet

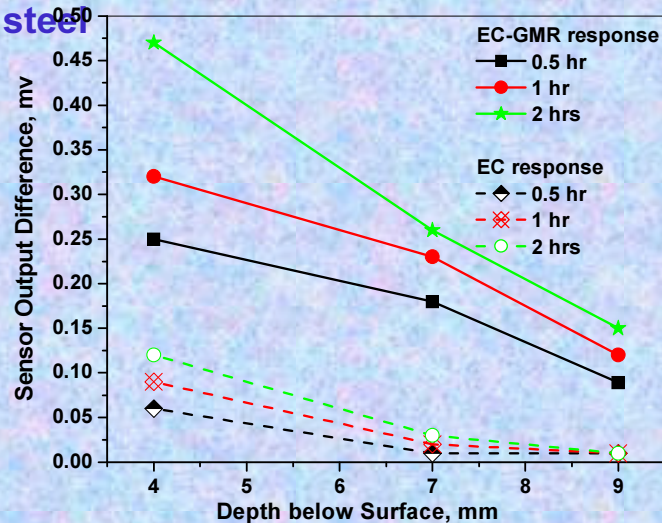
In-Service Inspection of stem generator



NDE for characterization of microstructures and degradation



Ultrasonic velocity ratio based characterisation of cold worked D9 steel



Eddy current-GMR for detection of intergranular corrosion in 304L steel

Detection and characterization

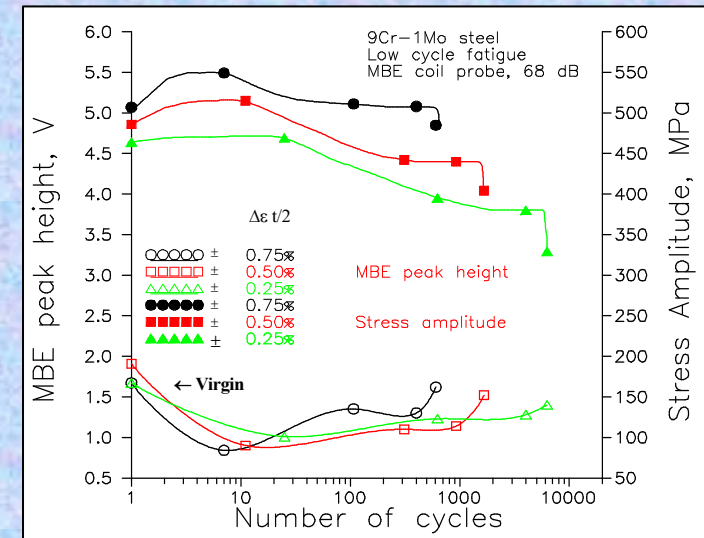
- Defects
- Microstructures
- Stresses

Variability -Challenges

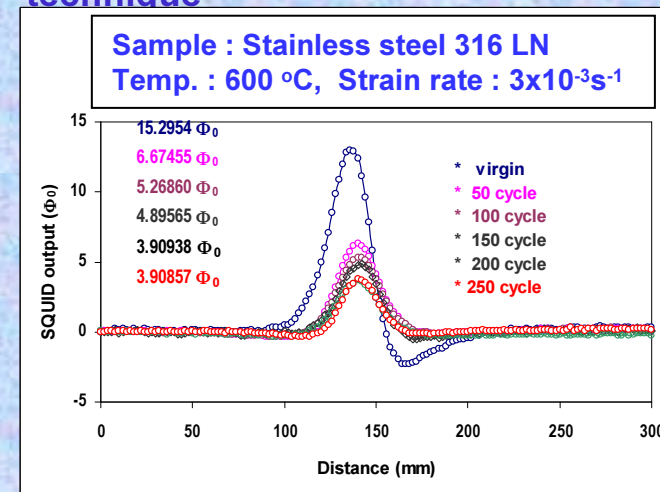
- Dimensions (nm-mm)
- Sensitivity
- Detectability (POD)
- Repeatability
- Operator based error
- Field implementation

Directions

- Sensor development
- Numerical modelling
- Automation
- In-situ monitoring
- Data fusion
- Intelligent NDE
- Sensor networks
- Miniaturization (phased-array)
- Wireless NDE
- Round robin tests
- Bench marking



Assessment of low cycle fatigue using Barkhausen emission technique

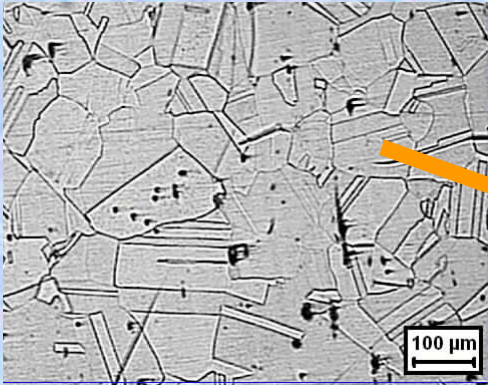


Early detection of fatigue damage in 316 LN welds using SQUIDs



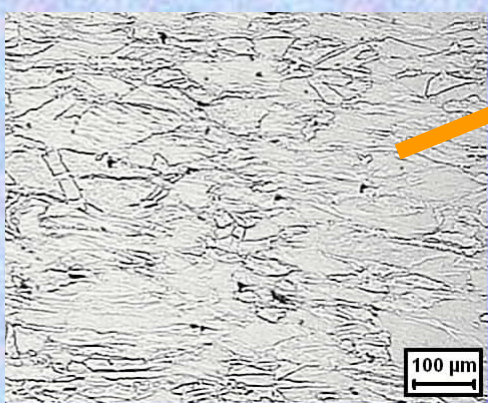
Ultrasonic C-Scan imaging of grain size variation in forged D9 alloy

190 VHN



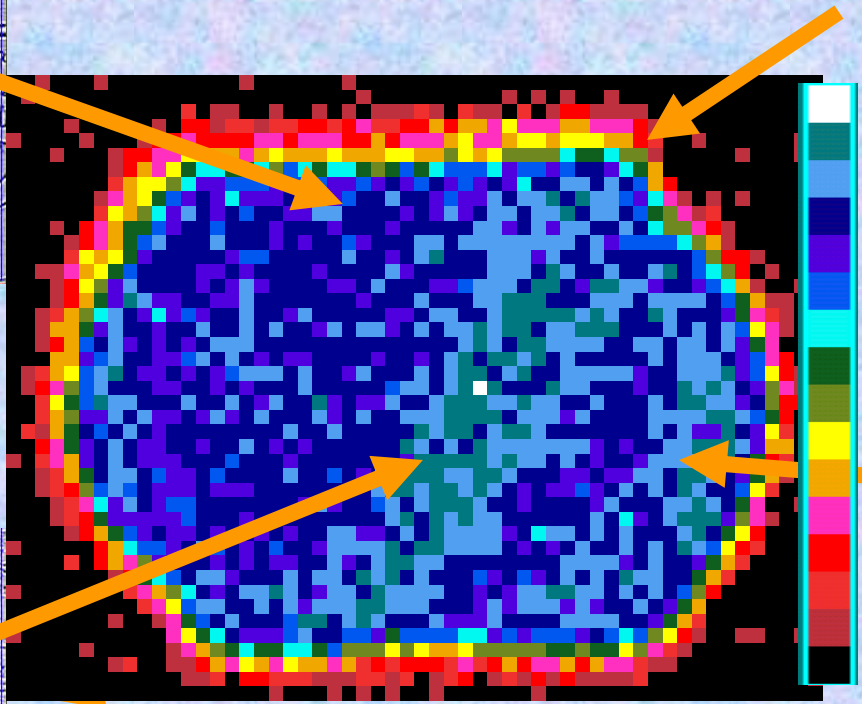
Coarse grains in dead metal zone

198 VHN



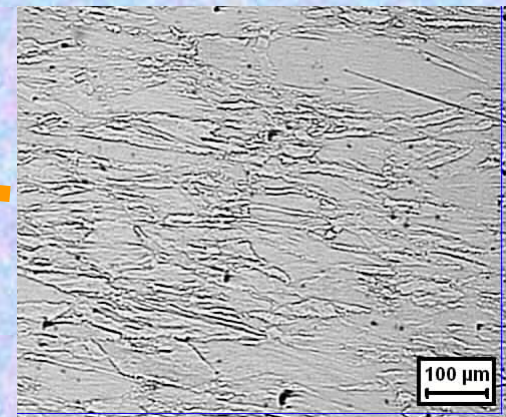
Fine grains in one shear band

Forged to 50%; 1273 K



Little skew in deformation

192 VHN

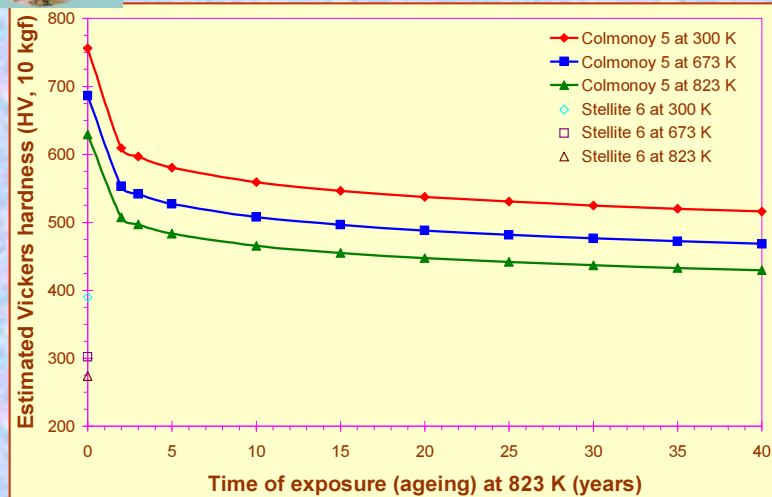


Fine grains in deformation zone

Variations in microstructures and forging conditions are monitored for quality assurance and process control



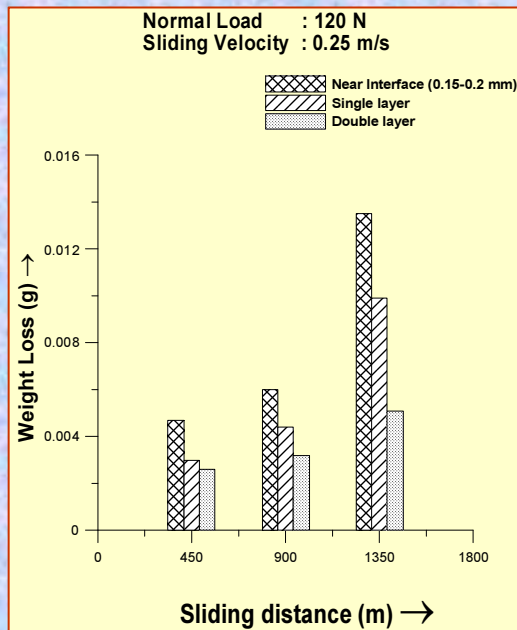
Hardfacing of PFBR Components: Basic Research to Technology



Predicted reduction in hardness with time



Hardfacing of PFBR Grid Plate



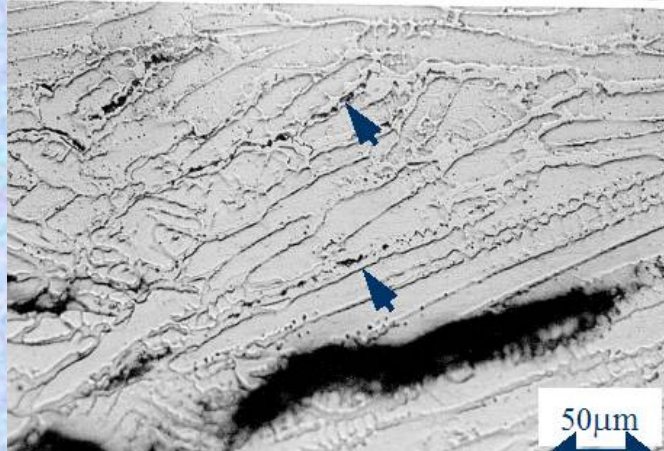
Effect of dilution on wear loss of the deposit

- Ageing studies on Ni base hardfacing alloys confirmed no significant deterioration in hardness with high temperature exposure.
- Hardness measurement, microstructural examination and wear tests confirmed significant reduction in properties by dilution from base metal. Hence, a minimum deposit thickness of 2 mm and Plasma Transferred Arc process were recommended.
- Hardfacing of 6 m diameter grid plate has been carried out without cracking by Mechanized Plasma Transferred Arc Process

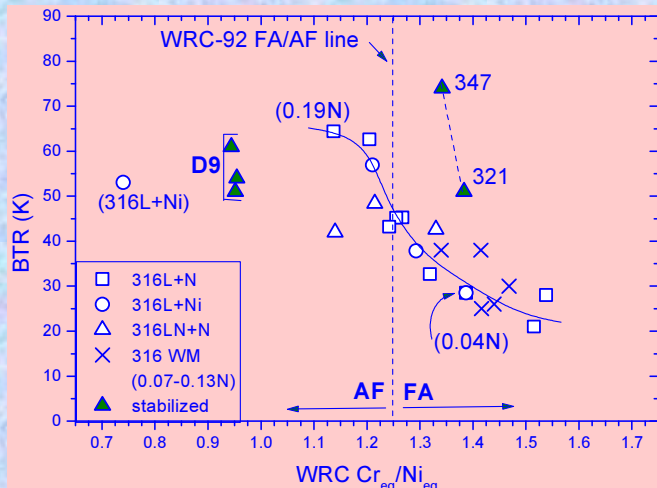
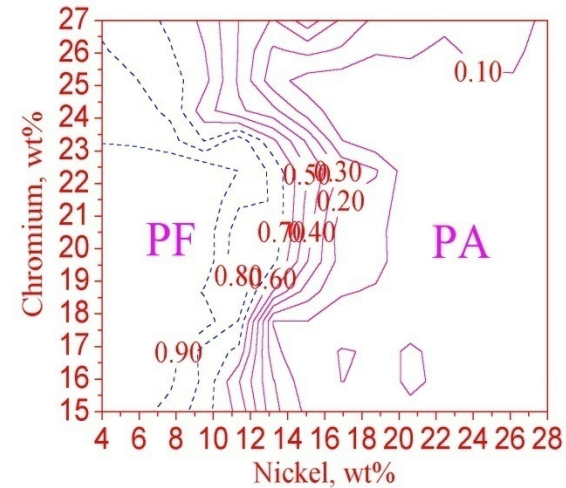
Hardfacing: A Technological Challenge in Reactor Component Fabrication



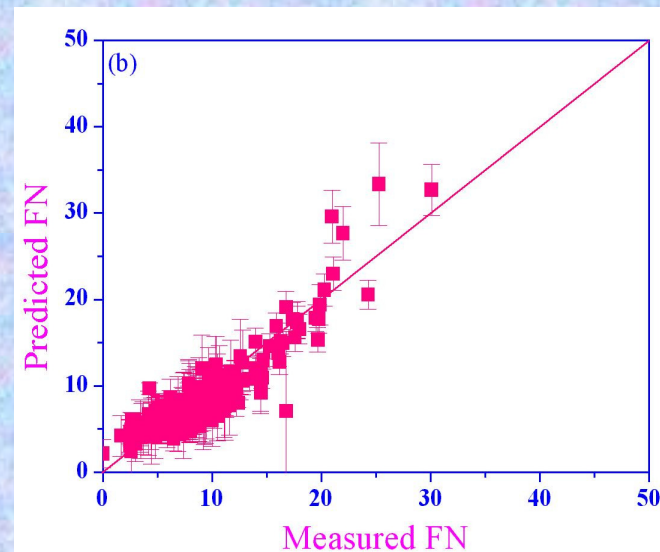
Weldability of Austenitic Stainless Steels - Hot-Cracking Susceptibility



Hot-cracking in Alloy D9 during Varcstraint testing



Weldability of austenitic SS base & weld for < 0.04%P+S



ANN modelling of delta ferrite to weld metal chemistry

Hot cracking Sensitivity of Reduced Activation Ferritic–Marensitic steels with varying Ta contents and optimizing the Chemical Composition of feed wire in TIG welding

Materials Issues to be Addressed

Austenitic Stainless Steels

- Heat-to-heat variation in the creep rupture properties (D9 and its variants)
- Generation on long-term creep & fatigue data to extend design life to 60 yrs
- Codification in standards (316 FR)

F/M Steels

- Heat-to-heat variation in the creep and swelling behavior
- Evaluation procedure of creep-fatigue interaction considering type IV cracking
- Optimization of specifications for enhanced high temperature resistance in sodium environment
- Development of manufacturing technology to fabricate large forgings and long thin double-walled heat exchanger pipes

ODS Steels

- Ferritic ODS steels suffer from anisotropy in microstructure
- Development of new welding procedures for F/M-ODS dissimilar welds (EM pulse, diffusion bonding, friction stir and explosive welding)
- Generating irradiation data and codification of the steels in standards
- Development of manufacturing technology for mass production
- Development and incorporation of advanced NDE techniques for manufacturing quality
- Improvement of corrosion resistance of 9Cr-ODS steels through development of smart & hard coatings and corrosion protection barriers
- Reduction of dissolution rates of 9Cr-ODS steels during reprocessing

Future Directions

- ✓ **Design based life-time performance** of plants in place of materials limited life of components
- ✓ **Need for high breeding ratio** and transmutation of long lived actinides necessitate evaluation of metallic fuel and reassessment of core component materials and back-end technologies.
- ✓ **Advanced NDE techniques** for enhanced manufactured quality and in-service damage assessment for enhanced safety
- ✓ **Multi-scale Modelling** will provide basis for physical understanding for the rationalisation of the experimental results, very much needed in consideration of the fact that the operating conditions of most future reactor concepts cannot be mimicked by any existing facility, so that extrapolation exercises will be eventually needed.
- ✓ **Converging to one F/M & ODS alloy system** for easy generation of irradiation data in a collaborative manner and for easy codification

EMERGING DOMAINS OF FUSION: SYNERGY WITH SFR TECHNOLOGY

- **Codes for High Temperature Design**
- **Liquid Metal Coolants**
- **ODS Steels**
- **Low Activation Steels for high irradiation environment**
- **Radiation Damage**
- **Coating & Joining technologies**
- **Manufacturing Technologies for Thick Components**
- **Grain Boundary Engineering for Enhancement of Mechanical Properties and Corrosion Resistance**
- **NDE for Characterization of microstructural changes and Monitoring of Mechanical Properties to ensure Structural Integrity**
- **Development of Sensors , ISI & Robotics**
- **Small Specimen Testing**
- **Enhancement in Simulation & Multiscale Modeling Expertise**

Baldev Raj and K. Bhanu Sankara Rao, 2009, Building on knowledge base of sodium cooled fast spectrum reactors to develop materials technology for fusion reactors, Journal of Nuclear Materials 386-388, pp. 935-943

K. Bhanu Sankara Rao, Baldev Raj, Ian Cook, Akira Kohyama and Sergei Dudarev, Materials Synergies between Fusion and Fast Spectrum Fission Systems, Proceedings of Eighth International symposium on Fusion Nuclear technology, ISFNT-8, Hiedleberg, Germany, Dec.2007, Nuclear Engineering & Design (In Press)

Fast Reactors for Energy Security



Science, Art, Literature and Philosophy belong to the whole world, and before them vanish the barriers of nationality